

---

# DIMENSION-ROBUST FUNCTION SPACE MCMC WITH NEURAL NETWORK PRIORS

---

**Torben Sell**

Statistical Laboratory  
Department of Pure Mathematics and Mathematical Statistics  
University of Cambridge, UK  
ts671@cam.ac.uk

**Sumeetpal S. Singh**

Signal Processing and Communications Laboratory  
Department of Engineering  
University of Cambridge, UK  
sss40@cam.ac.uk

June 30, 2022

## ABSTRACT

This paper introduces a new prior on functions spaces which scales more favourably in the dimension of the function's domain compared to the usual Karhunen-Loève function space prior, a property we refer to as *dimension-robustness*. The proposed prior is a Bayesian neural network prior, where each weight and bias has an independent Gaussian prior, but with the key difference that the variances decrease in the width of the network, such that the variances form a summable sequence and the infinite width limit neural network is well defined. We show that our resulting posterior of the unknown function is amenable to sampling using Hilbert space Markov chain Monte Carlo methods. These sampling methods are favoured because they are stable under mesh-refinement, in the sense that the acceptance probability does not shrink to 0 as more parameters are introduced to better approximate the well-defined infinite limit. We show that our priors are competitive and have distinct advantages over other function space priors. Upon defining a suitable likelihood for continuous value functions in a Bayesian approach to reinforcement learning, our new prior is used in numerical examples to illustrate its performance and dimension-robustness.

**Keywords** Bayesian Neural Networks · Value Function Estimation · preconditioned Crank Nicolson · Langevin Dynamics · Bayesian Reinforcement Learning

## 1 Introduction

Generating samples from probability measures on function spaces is both a challenging computational problem and a very useful tool for many applications, including mathematical modelling in bioinformatics [Quarteroni et al., 2017], data assimilation in reservoir models [Iglesias et al., 2013], and velocity field estimation in glaciology [Minchew et al., 2015], amongst many others. This paper addresses the problem of defining a computationally and statistically favourable function space prior.

In Bayesian inference on separable Hilbert spaces [Stuart, 2010], many posterior measures  $\pi$  are absolutely continuous with respect to their prior  $\mu_0$  (often a Gaussian measure, see Knapik et al. [2011] and Dashti et al. [2013], but not always, see Dashti et al. [2011], Hosseini [2017], and Hosseini and Nigam [2017]), with the likelihood acting as the Radon-Nikodym derivative  $d\mu/d\mu_0 \propto \mathcal{L}$ . When the priors are Gaussian measures, truncating their Karhunen-Loève expansions reduces the problem of sampling from infinite-dimensional measures to sampling from a finite-dimensional parameter space. This approximation to the true posterior gets better by including more parameters in the truncated expansion. The practical applicability of these priors are, however, restricted to inferring unknown functions with

low-dimensional domain, as the orthogonal basis required results in the complexity scaling exponential with the dimension of the unknown function’s domain.

Another approach to define function space priors are Bayesian Neural Networks (BNNs) [Neal, 1995, 2012] which drew a lot of attention in the machine learning community over the past years. These priors are obtained by placing a prior distribution over the weights and biases of a neural network, with the default choice being a centered Gaussian prior on the weights with variances that scale as  $\mathcal{O}(1/N^{(l)})$ , where  $N^{(l)}$  is the number of nodes in layer  $l$ . Although some theoretical results exist [Matthews et al., 2018], popular criticisms include the lack of interpretability of the resulting BNNs, and recent work [Wenzel et al., 2020] has highlighted inter alia that novel priors are needed. Sampling approaches include Hamiltonian Monte Carlo [Neal, 1995], and more advanced integrators [Leimkuhler et al., 2019]; However, inference is often limited to finding the maximum-a-posteriori (MAP) estimate of the posterior [Welling and Teh, 2011], and one cannot easily expand the parameter space to obtain more accurate estimates as is the case for the Karhunen-Loève expansion: one would either have to adjust the prior variances for all nodes within the amended layer, or have to deal with exploding functions.

Other popular function space priors include Deep Gaussian Processes [Damianou and Lawrence, 2013], for which few theoretical results [Dunlop et al., 2018] are known. These can not be straight forwardly used in conjunction with Hilbert space MCMC techniques which is the focus of this work, and we thus omit a discussion thereof.

To calculate expectations with respect to the respective posteriors, computational methods are required as the integrals are usually not analytically tractable. Two popular sampling algorithms for posteriors defined on Hilbert spaces are the preconditioned Crank-Nicolson (pCN) algorithm and its likelihood-informed counterpart the preconditioned Crank-Nicolson Langevin (pCNL), which arise from clever (and in a way optimal) discretisations of certain stochastic differential equations [Cotter et al., 2013], are asymptotically exact, and are dimension-independent in the sense that their step-size does not depend on the discretisation [Hairer et al., 2014, Eberle et al., 2014]. This stands in stark contrast to the well-known dimensional-dependent scaling of popular MCMC algorithms such as Random Walk Metropolis and Metropolis Adjusted Langevin Algorithm [Roberts and Rosenthal, 1998, Roberts et al., 2001]. Practical implementations of pCN and pCNL exploit the equivalence of Gaussian measures and the Karhunen-Loève (KL) expansion which holds under fairly general assumptions. Owing to the orthogonality of the basis in the KL expansion, these methods come with a variety of theoretical results, such as concentration inequalities and contraction rates, see e.g. Agapiou et al. [2013], Nickl and Giordano [2020], Knapik et al. [2011], van der Vaart et al. [2008]. Geometric [Beskos et al., 2017] and likelihood-informed [Cui et al., 2016] modifications of pCNL can reduce the computational cost provided one knows which basis functions are informed by the data, but they can not circumvent the costly scaling in the domain dimension. This is presumably the main reason why these methods have rarely been used for inferring unknown functions with domains larger than dimension two (i.e.  $\mathbb{R}^2$ ) in reported examples in the literature.

This paper introduces a new neural network based prior, coined *trace-class* neural network priors, which allows for scalable (in the domain dimension) Bayesian function space inference. Hilbert space MCMC algorithms are then used to sample from the resulting posteriors, and owing to their stability under mesh-refinement, enhances the practical utility of our framework. In addition to comparisons with reported examples in the literature, we also demonstrate our technique’s usefulness on a challenging 17-dimensional reinforcement learning example where the aim is to learn control strategies via a Bayesian formulation.

The main contributions of this paper are as follows:

- We introduce a *trace-class* prior for neural networks, and demonstrate its practical utility. The prior is independent, centred, and Gaussian across weights but is non-exchangeable over the weights within each layer and has a summable variance sequence. The latter ensures it is a valid prior for an infinite width network, while the former results in parameters being better identified from an inference perspective. We further prove that this prior is appropriate for use with Hilbert space MCMC methods even in the infinite-width limit (Theorem 1), and is thus suitable for application to problems with high-dimensional state spaces owing to the inherent scalability of neural networks to its number of inputs.
- We propose a suitable likelihood for Bayesian Reinforcement Learning (BRL) for inferring the unknown continuous state value function that best describes an observed state-action data sequence. Theorem 2 and Lemma 1 justify the use of this likelihood with Gaussian prior measures on function spaces, and with our proposed neural network prior. This likelihood is also potentially of interest to the machine learning community in its own right.
- We apply Hilbert space MCMC methods to infer the unknown optimal value function in two continuous state control problems, using both our new prior and likelihood function. We provide numerical evidence that, in contrast to standard function space priors, the trace-class neural network prior is scalable to higher dimensional problems.

The rest of this paper is organised as follows: In Section 2 we introduce the general inference problem, describe the canonical approximation for functions on  $\mathbb{R}^d$ , describe MCMC methods on an infinite-dimensional Hilbert space including their construction and the assumptions under which these methods are well-defined. Section 3 introduces the

trace-class neural network prior and states one of our main theoretical results, showing that the proposed prior satisfies the necessary assumptions to be used with a Hilbert space MCMC algorithm. In Section 4 we state the Bayesian Reinforcement Learning (BRL) problem and introduce the likelihood to be used for inferring continuous state value functions from state-action data. We then show that the likelihood satisfies the assumptions needed to be admissible in a Hilbert space MCMC setting. Finally, Section 5 provides numerical results for the proposed prior and the likelihood for different control problems. Proofs can be found in the appendix.

### 1.1 Notation

We use curly letters ( $\mathcal{X}$  and  $\mathcal{A}$ ) for spaces and sets. Subscripts denote both time and spatial variables, but it will be clear from the context which ones we are considering. Value functions are denoted with the letter  $v$  throughout, and in Section 2.2 we follow the notation introduced by Cotter et al. [2013].

$\Phi$  denotes the Gaussian cumulative distribution function (cdf),  $\phi$  the Gaussian probability density function (pdf).  $\varphi$  is used for either a basis function (in the context of basis expansions) or, in the the context of neural networks, as an activation function. It will be clear from the context which of the two we are considering. The likelihood function we will write as  $\mathcal{L}$ , the log-likelihood as  $\ell$ .  $\ell^2$  also denotes the space of square-summable sequences, and further the space of square-integrable functions from  $\mathcal{X} \subseteq \mathbb{R}^d$  to  $\mathbb{R}$  is denoted  $L^2(\mathcal{X}, \mathbb{R})$  or simply  $L^2$ .

## 2 Problem Formulation

The objective is to sample from a target distribution  $\mu$  defined over an infinite dimensional separable Hilbert space. The targets of interest in this work are Bayesian posterior distributions arising from a Gaussian prior measure  $\mu_0$  and a likelihood which can be evaluated point wise. One such likelihood is a Gaussian likelihood given by observations of a PDE solution such as in Section 3.2.1, one for continuous control problems will be introduced in Section 4. In what follows, we will assume that the posterior has a density with respect to the prior, in which case the Radon-Nikodym derivative is well defined and the posterior density with respect to the prior is given by

$$\frac{d\mu}{d\mu_0}(u) = \frac{1}{Z} \exp(\ell(y|u)),$$

where  $\ell$  is the log-likelihood, and  $Z = \int \exp(\ell(y|u))\mu_0(du)$  is the normalisation constant. **Remark:** Stuart [2010] shows that the likelihood arising from Gaussian observations of forward solutions of certain PDEs satisfies this, our Theorem 2 shows that the likelihood arising in stochastic control problems also satisfies this.

For any such infinite-dimensional separable Hilbert space  $\mathcal{H}$ , say  $\mathcal{H} = L^2(\mathcal{X}, \mathbb{R})$  to frame the discussion in this section (or later on in Section 3 the sequence space  $\mathcal{H} = \ell^2$ ), there exists an orthonormal basis  $\{\varphi_i\}_{i=1}^\infty$  such that any element  $u \in \mathcal{H}$  can be obtained as the limit  $u(x) = \lim_{N \rightarrow \infty} \sum_{i=1}^N a_i \varphi_i(x)$ , where  $a_i = \langle u, \varphi_i \rangle_{\mathcal{H}}$ . Let the prior  $\mu_0 = \mathcal{N}(0, \mathcal{C})$  be a Gaussian measure on  $\mathcal{H}$ . If the operator  $\mathcal{C}$  is trace-class with orthonormal eigenvalue-eigenfunction pairs  $(\lambda_i^2, \varphi_i(x))$ ,  $i = 1, 2, \dots$ , one can sample from  $\mu_0$  by sampling a sequence of  $\xi_i \sim \mathcal{N}(0, \lambda_i^2)$  and by then defining

$$u(x) = \sum_{i=1}^{\infty} \xi_i \varphi_i(x). \tag{1}$$

This is the Karhunen-Loève (KL) expansion [Giné and Nickl, 2016]. One may thus think of a sample from the Gaussian measure as the sum of a sequence of 1-dimensional Gaussians with summable variances<sup>1</sup>. This allows us to truncate the series expansion such that we have  $N$  active terms, with the remainder giving an estimate for the approximation error:

$$u(x) = \sum_{i=1}^N \xi_i \varphi_i(x) + \sum_{i=N+1}^{\infty} \xi_i \varphi_i(x), \quad \|u(x) - \sum_{i=1}^N \xi_i \varphi_i(x)\| \leq \sum_{i=N+1}^{\infty} \|\xi_i \varphi_i(x)\|.$$

Other more elaborate truncation schemes are discussed in Cotter et al. [2013], but we will focus on a fixed number of terms for computational and notational convenience. For some applications,  $\varphi_i$  for large  $i$  can be interpreted as high-oscillating functions which may not be discernible by the observation operator, see the example in Section 3.2.1. We emphasise that the above discussion holds not only for the space  $\mathcal{H} = L^2(\mathcal{X}, \mathbb{R})$ , which is predominantly how it is applied in Beskos et al. [2008], Cotter et al. [2013], Beskos et al. [2017], but also for  $\mathcal{H} = \ell^2$ , which will be of particular importance in this paper. In infinite-dimensional spaces, one has to be careful to ensure the posterior is well defined, see Stuart [2010] for a discussion on Gaussian priors and likelihoods given through possibly non-linear mappings, observed in Gaussian noise. We will work with the following assumptions, which we prove are satisfied for the likelihood defined in Section 4.

1.  $\mu_0$  is a Gaussian prior defined on a separable Hilbert space  $\mathcal{H}$ , with a trace-class covariance operator  $\mathcal{C}$ , that is, the eigenvalues  $\lambda_i^2$  corresponding to the eigenfunctions  $\varphi_i$  satisfy  $\sum_i \lambda_i^2 < \infty$ ;
2. The posterior is well-defined, i.e. the integral of the likelihood with respect to the prior is positive and finite.

<sup>1</sup>If the variances are not summable, the sum in (1) diverges with positive probability.

## 2.1 A canonical approximation for functions on $\mathbb{R}^d$

Consider a  $d$ -dimensional hypercube  $\mathcal{X} = [0, 1]^d$ , the Hilbert space  $\mathcal{H} = L^2(\mathcal{X}, \mathbb{R})$ , and a Gaussian prior measure  $\mu_0$  on  $\mathcal{H}$ . A Bayesian approach entails choosing the covariance matrix  $\mathcal{C}$  for the prior  $\mu_0$ , and we discuss a canonical choice below. If the problem requires it, as in Section 3.2.1 where a PDE is solved, it is possible to choose  $\mathcal{C}$  such that the samples are almost surely differentiable.

One problem with this approach is that it scales badly with dimension: say one has eigenvalues  $\lambda_i$  and basis functions  $\varphi_i$  for a 1-dimensional function, and truncates the KL expansion (1) after  $N$  terms. The easiest way to scale this basis up to a  $d$ -dimensional domain is by taking a tensor product of the basis, see e.g. Iserles and Nørsett [2009] for the multivariate Fourier basis, or Wojtaszczyk [1997] for Wavelets and other basis expansions. For the KL expansion, we thus get, for a multi-index  $k = (k_1, \dots, k_d)$  with  $k_i = 1, \dots, N$ ,

$$u(x) = \sum_k \xi_k \varphi_k(x) = \sum_{k_1=1}^N \cdots \sum_{k_d=1}^N \xi_{k_1, \dots, k_d} (\varphi_{k_1}(x_1) \cdots \varphi_{k_d}(x_d)), \quad (2)$$

where  $\xi_{k_1, \dots, k_d} \sim \mathcal{N}(0, \lambda_{k_1, \dots, k_d}^2)$  with  $\lambda_{k_1, \dots, k_d}$  being a function of the respective eigenvalues  $\lambda_{k_i}$  capturing the correlation between dimensions. In total, there are  $N^d$  active terms, that is, the complexity is exponential in the dimension  $d$ . This will be computationally prohibitively expensive, even for moderately small  $d$ .

To circumvent the exponential cost in the domain dimension, one may want to exploit any knowledge of independence that one knows of. Assume, for example, that the function of interest can be approximated as  $u(x) \approx v_0 + \sum_{i=1}^d u_i(x_i)$  with  $u_i : [0, 1] \rightarrow \mathbb{R}$ ,  $\int u_i(x_i) dx_i = 0$ . With this approximation, the number of terms to be inferred is linear in  $d$ . In practice, this is often oversimplifying. More generally, one can use approximations including higher order functions following Sobol [1993], e.g.

$$u(x) \approx \sum_{i=1}^d u_i(x_i) + \sum_{i=1}^d \sum_{j=i+1}^d u_{i,j}(x_i, x_j), \quad (3)$$

with  $dN + \frac{d(d-1)}{2}N^2$  coefficients to be estimated. Using such an approximation can achieve a massive dimension reduction, avoiding the inference of all  $N^d$  coefficients, but requires good knowledge of the properties of the quantities of interest. With the approximation (3) in mind, one restricts oneself to the prior on finitely many random functions  $u_i$  and  $u_{i,j}$ , each of which themselves is sampled from a Gaussian measure  $\mathcal{N}(0, \mathcal{C}_1)$ , or  $\mathcal{N}(0, \mathcal{C}_2)$ , respectively. One identifies each of these functions with their Karhunen-Loève expansion

$$u_i(x_i) = \sum_{k=1}^{\infty} \xi_{i,k} \varphi_k(x_i), \quad u_{i,j}(x_{i,j}) = \sum_{k=1}^{\infty} \xi_{i,j,k} \psi_k(x_i, x_j) \quad (4)$$

where the  $\varphi_k$  and  $\psi_k$  are the eigenfunctions corresponding to the eigenvalues  $\lambda_{\varphi,k}^2$  and  $\lambda_{\psi,k}^2$ , respectively. The  $\xi_{i,k}$  and  $\xi_{i,j,k}$  are independent normal random variables  $\xi_{i,k} \sim \mathcal{N}(0, \lambda_{\varphi,k}^2)$  and  $\xi_{i,j,k} \sim \mathcal{N}(0, \lambda_{\psi,k}^2)$ . As before one requires the covariance operators to be *trace-class*, and truncates the expansion (4) after a finite number of term.

The numerical experiments using the KL function space prior in this paper are based on the following Fourier basis functions,  $\varphi_k$  defined on  $[0, 1]$ ,  $\psi_k = \psi_{k_1, k_2}$  defined on  $[0, 1]^2$  and indexed by a double index  $k = (k_1, k_2)$ :

$$\begin{aligned} \varphi_{2k}(x_i) &= \sin(2\pi k x_i) \\ \varphi_{2k+1}(x_i) &= \cos(2\pi k x_i) \\ \psi_{2k_1, 2k_2}(x_i, x_j) &= \varphi_{2k_1}(x_i) \varphi_{2k_2}(x_j) = \sin(2\pi k_1 x_i) \sin(2\pi k_2 x_j) \\ \psi_{2k_1+1, 2k_2}(x_i, x_j) &= \varphi_{2k_1+1}(x_i) \varphi_{2k_2}(x_j) = \cos(2\pi k_1 x_i) \sin(2\pi k_2 x_j) \\ \psi_{2k_1, 2k_2+1}(x_i, x_j) &= \varphi_{2k_1}(x_i) \varphi_{2k_2+1}(x_j) = \sin(2\pi k_1 x_i) \cos(2\pi k_2 x_j) \\ \psi_{2k_1+1, 2k_2+1}(x_i, x_j) &= \varphi_{2k_1+1}(x_i) \varphi_{2k_2+1}(x_j) = \cos(2\pi k_1 x_i) \cos(2\pi k_2 x_j), \end{aligned} \quad (5)$$

for  $i \neq j$ , with corresponding eigenvalues

$$\lambda_{\varphi, 2k}^2 = \lambda_{\varphi, 2k+1}^2 = \frac{1}{k^\alpha}, \quad \lambda_{\psi, 2k_1, 2k_2}^2 = \lambda_{\psi, 2k_1+1, 2k_2}^2 = \lambda_{\psi, 2k_1, 2k_2+1}^2 = \lambda_{\psi, 2k_1+1, 2k_2+1}^2 = \frac{1}{(\sqrt{k_1^2 + k_2^2})^\alpha}. \quad (6)$$

See Figure 1 for some representative draws from this prior.

Approximations such as (3) require a good understanding of the functions of interest, which is generally overly restrictive: the statistician or researcher needs to have a good understanding about which coefficients of the eigen expansion are informed by the likelihood, and should therefore be included in the analysis. Section 3 will introduce a prior which scales favourably with the domain-dimension as it does not require pre-defining an orthogonal basis.

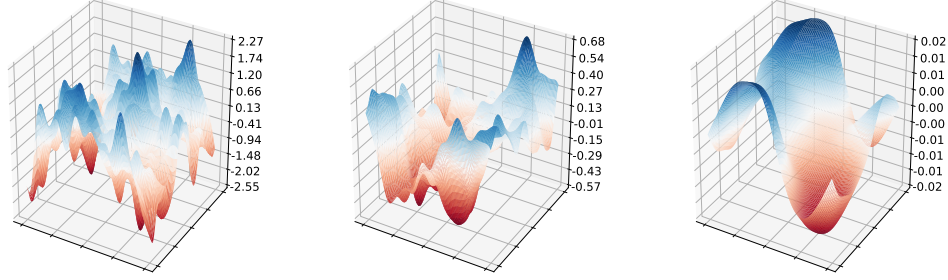


Figure 1: Three samples from the Karhunen-Loève prior; the basis functions are the two-dimensional Fourier functions. In ascending order from left to right we set  $\alpha \in \{1.001, 1.5, 3\}$  with the eigenvalues scaling as  $\lambda_k^2 \propto 1/(k_1^2 + k_2^2)^\alpha$ , for the double index  $k = (k_1, k_2)$ . The tuning parameter  $\alpha$  controls the smoothness of the samples.

## 2.2 Metropolis-Hastings algorithms on Hilbert spaces

This section recapitulates how to define ‘sensible’ Metropolis-Hastings Markov chain Monte Carlo algorithms for inference over the  $\xi_i$  in (1). The use of Markov chains is a popular approach to sample from distributions on finite-dimensional state spaces (see Brooks et al. [2011] for an overview of MCMC methods). Here, we review algorithms which can theoretically deal with arbitrarily many basis coefficients, without the usual problem of the acceptance probability degenerating as one includes more coefficients. This property, known as *stability under mesh-refinement*, is not satisfied by the popular Random Walk Metropolis algorithm (RWMH, Hastings [1970]), or by the Metropolis Adjusted Langevin Algorithm (MALA, Roberts et al. [1996]).

Two algorithms which are both dimension-independent are the preconditioned Crank-Nicolson (pCN) and the preconditioned Crank-Nicolson Langevin (pCNL) algorithms, the former introduced as early as Neal [1998] and both derived and discussed in Cotter et al. [2013], see also Beskos et al. [2008], Rudolf and Sprungk [2018], Beskos et al. [2017] for further reading and generalisations. Motivated by the idea of increasing dimensions translating to evaluating a function on a finer mesh, we refer to the dimension-independence of these algorithms as *stability under mesh-refinement*. Both algorithms can be seen as a discretisation of the following stochastic partial differential equation:

$$\frac{du}{ds} = -\mathcal{K}(C^{-1}u - \gamma D\ell(u)) + \sqrt{2\mathcal{K}}\frac{dB}{ds}, \quad (7)$$

where  $D\ell$  is the Fréchet derivative of the log-likelihood<sup>2</sup>,  $\mathcal{K}$  is a preconditioner,  $C$  is the covariance operator of the Gaussian prior measure,  $B$  is a Brownian motion, and  $\gamma$  a tuning parameter: if  $\gamma = 0$ , the invariant distribution of (7) is the prior  $\mu_0$ , and for  $\gamma = 1$  the invariant distribution is the posterior  $\mu$ . With the choice  $\mathcal{K} = C$  (the preconditioned case, such that the dynamics are scaled to the prior variances), discretising (7) using a Crank-Nicolson scheme results in pCN (for  $\gamma = 0$ ) and pCNL (for  $\gamma = 1$ ). The resulting discretisations can be simplified to

$$v = \sqrt{1 - \beta^2}u + \beta w, \quad w \sim \mathcal{N}(0, C), \quad (\text{pCN}) \quad (8)$$

$$v = \frac{1}{2 + \delta} \left[ (2 - \delta)u + 2\delta C D\ell(u) + \sqrt{8\delta}w \right], \quad w \sim \mathcal{N}(0, C), \quad (\text{pCNL}) \quad (9)$$

for step sizes  $\beta \in (0, 1]$  and  $\delta \in (0, 2)$ , respectively. Note that due to the discretisation scheme used, pCN is prior-reversible, and using it as a proposal in a Metropolis-Hastings sampler to target the posterior, the proposal is accepted with probability  $\min\{1, \exp(-\ell(u) + \ell(v))\}$ . If the pCNL dynamics are used as a proposal for a MH scheme, the acceptance probability is given by  $\min\{1, \exp(\rho(u, v) - \rho(v, u))\}$  where

$$\rho(u, v) = -\ell(u) - \frac{1}{2}\langle v - u, D\ell(u) \rangle - \frac{\delta}{4}\langle u + v, D\ell(u) \rangle + \frac{\delta}{4}\|\sqrt{C}D\ell(u)\|^2.$$

Both pCN and pCNL are such that, for an uninformative likelihood, all moves are accepted. In practice, the likelihood assumptions 3 and 4 ensure that, unlike RWMH or MALA, neither pCN nor pCNL require their step size  $\beta$  or  $\delta$  to go to 0 as one includes more coefficients in the KL expansions [Cotter et al., 2013].

<sup>2</sup>Note that we use the log-likelihood  $\ell$  rather than the potential  $\Phi = -\ell$  as the authors of Cotter et al. [2013].

For mathematical completeness, we emphasise that in order to ensure that the processes arising from the above defined transition kernels have the desired stationary distribution, one needs to check that they yield a strong aperiodic, recurrent Harris chain (giving the existence of a unique stationary distribution Athreya and Ney [1978]), and satisfy the detailed balance condition (showing that the stationary distribution is the one of interest Tierney et al. [1998]).

To conclude this section, we state the assumptions [Cotter et al., 2013, Assumptions 6.1] under which both pCN [Cotter et al., 2013, Thm 6.2] and pCNL (see Theorem 4 in the appendix) are well defined, where Assumption 5 is only required for pCNL [Beskos et al., 2017]:

3. There exist constants  $K > 0, p > 0$  such that  $0 \leq -\ell(y|u) < K(1 + \|u\|^p)$  holds for all  $u \in \mathcal{H}$ ;
4.  $\forall r > 0 \exists K(r) > 0$  such that for all  $u, v$  with  $\max(\|u\|, \|v\|) < r$ :

$$|\ell(y|u) - \ell(y|v)| \leq K(r)\|u - v\|;$$

5.  $\forall u \in \mathcal{H}: \mathcal{CD}\ell \in \text{Im}(\mathcal{C}^{1/2})$ , that is, the *preconditioned* differential operator is in the support of the prior with probability 1.

### 3 Trace-Class Neural Network Priors

The Gaussian prior on  $\mathcal{H} = L^2(\mathcal{X}, \mathbb{R})$  exploits the isometry between the function space  $L^2(\mathcal{X}, \mathbb{R})$  and the sequence space  $\ell^2$  using the Karhunen-Loève expansion [Giné and Nickl, 2016], but the computational complexity of using a basis-expansion on a high-dimensional domain is unfeasible even when using approximate function representations such as in Sobol [1993].

Neural networks have shown excellent empirical performance in high-dimensional function regression tasks, and Bayesian neural networks (BNNs) use their architecture to define priors over such functions. BNNs are popular as they empirically show good results, and are computationally fast. While some theoretical results are known [Hornik, 1991, Matthews et al., 2018], the interpretability of the posteriors arising from Bayesian neural networks are limited, and priors are often understood as a regularisation method in optimisation [Welling and Teh, 2011], rather than the actual prior belief one has on the weights; see also Lipton [2018] for a broader discussion of interpretability.

We now propose a prior that is also defined over the parameters  $\theta$  of the neural network, but is, in contrast to existing priors for neural networks, well-defined in the infinite-width limit. As inference is done over the parameters which form a countable sequence, the Hilbert space of interest is  $\mathcal{H} = \ell^2$ , the space of square-summable sequences, for which the dimension-independent MCMC methods discussed in Section 2.2 are applicable. Through the architecture of the neural network, the prior  $\mu_0$  over the parameters implicitly defines a prior on the output function of the neural network. Under mild assumptions on the network architecture, and if  $\mathcal{X}$  is compact, the output functions  $v_\theta$  are  $\mu_0$ -almost surely square-integrable over  $\mathcal{X}$ , and the prior thus naturally defines a prior over  $L^2(\mathcal{X}, \mathbb{R})$  as well. The proposed prior is also more flexible than the Karhunen-Loève expansion of a Gaussian measure: one needs not to specify a covariance operator and find its eigenfunctions. By giving up the orthogonality of these eigenfunctions which allow for a rich theoretical analysis, one gains on the performance side. We coin the term *trace-class neural network prior* to emphasise that the prior leads to a well-defined function space prior if the variances of all parameters are appropriately summable. The term is well-established for Gaussian measures, where these are called trace-class if the eigenvalues of the covariance operator are summable.

To set the scene, consider a  $n$ -layer feed-forward fully-connected neural network. Let  $\alpha > 1$  be a fixed constant, and let  $\sigma_{w_l}^2, \sigma_{b_l}^2 \in \mathbb{R}^+$  for  $l = 1 \dots n + 1$ . The layer width of layer  $l$  is  $N^l$ , the input is  $x \in [0, 1]^d$ , and the output is  $v(x) = f_1^{(n+1)}(x) \in \mathbb{R}$ ; for notational convenience we write  $N^0 = d$  and  $N^{n+1} = 1$ . The network is described fully but the set of weights and biases,

$$w = \left\{ w_{i,j}^{(l)} \right\}_{i=1, j=1, l=1}^{N^l, N^{l-1}, n+1}, \quad b = \left\{ b_i^{(l)} \right\}_{i=1, l=1}^{N^l, n+1}, \quad \theta = (w, b), \quad (10)$$

where we have summarised  $w$  and  $b$  as  $\theta$ . The prior  $\mu_0$  is now defined as follows: the individual weights and biases in each layer  $l$  are independent and normally distributed, and we emphasise here that the novelty is to choose the variances not uniformly, but to decrease them as one moves into the tail nodes:

$$W_{i,j}^{(1)} \sim \mathcal{N}\left(0, \frac{\sigma_{w^{(1)}}^2}{i^\alpha}\right), \quad W_{i,j}^{(l)} \sim \mathcal{N}\left(0, \frac{\sigma_{w^{(l)}}^2}{(ij)^\alpha}\right) \text{ for } l = 2 \dots n + 1, \quad B_i^{(l)} \sim \mathcal{N}\left(0, \frac{\sigma_{b^{(l)}}^2}{i^\alpha}\right), \quad (11)$$

where  $i, j$ , and  $l$  range over the obvious indices, cf. (10). The reader should note that the prior is invariant with respect to permutation of the input variables, thus avoiding preferential treatment of any of the inputs.

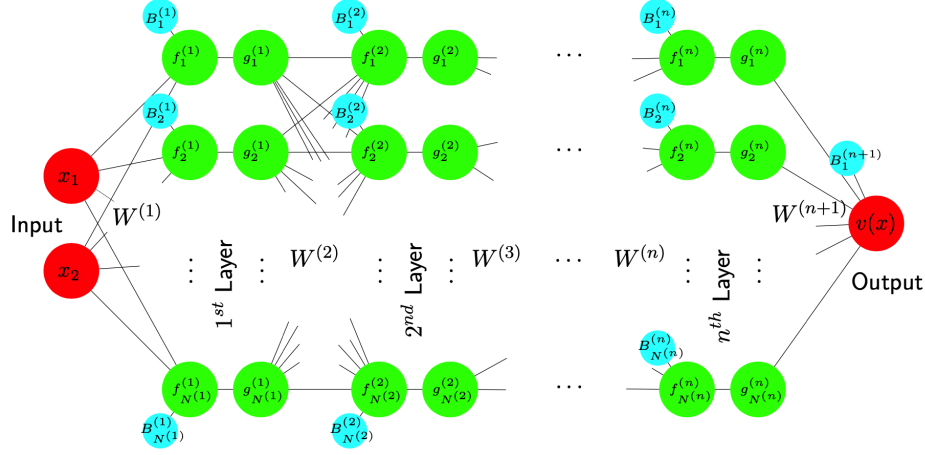


Figure 2: A  $n$ -layer feed-forward neural network, used to define a function  $v : \mathbb{R}^2 \rightarrow \mathbb{R}$ . Note that  $g_i^{(l)} = \varphi(f_i^{(l)})$ .

Given an *activation function*  $\varphi : \mathbb{R} \rightarrow \mathbb{R}$ , we define the random functions in the respective layers by

$$\begin{aligned} f_i^{(1)}(x) &= b_i^{(1)} + \sum_{j=1}^d w_{i,j}^{(1)} x_j, \quad i = 1 \dots N^1 \\ f_i^{(l)}(x) &= b_i^{(l)} + \sum_{j=1}^{N^{l-1}} w_{i,j}^{(l)} \varphi(f_j^{(l-1)}(x)), \quad i = 1 \dots N^l, l = 2 \dots n \\ v(x) &= f_1^{(n+1)}(x) = b_1^{(n+1)} + \sum_{j=1}^{N^n} w_{1,j}^{(n+1)} \varphi(f_j^{(n)}(x)), \end{aligned} \quad (12)$$

see Figure 2 for an illustration.

The tuning parameter  $\alpha$  controls how much information one believes concentrates on the first nodes. If  $\alpha > 1$  we refer to the prior as *trace-class*, coining the term *trace-class neural network priors*. If one believes that many nodes are important, one should choose  $\alpha$  close to 1, larger values of  $\alpha$  result in strong concentration of information on the first nodes. See Figure 3 for three representative draws from the neural network prior. As the next theorem will show, this allows indeed to define an infinitely wide network by taking  $N^l = \infty$ , and the variances can be summarised in a diagonal covariance operator  $\mathcal{C}$ ; this prior is well-defined on an infinite-dimensional Hilbert space (isometric to  $\ell^2$ ), and can thus be used in the algorithms from Section 2. In practice, one truncates the number of nodes within each layer as for the priors described before, or one may randomly switch nodes on and off similarly to the random truncation prior used in Cotter et al. [2013].

In what follows, we will often write  $v(x) = v_\theta(x)$  to emphasise the dependence of the function samples on the weights and biases. In order to be able to interpret the samples, we generally want the prior to satisfy the following desirable properties:

6.  $\forall x \in [0, 1]^d$  one has  $|f_i^{(l)}(x)| < \infty$   $\mu_0$ -almost surely,  $\mathbb{E} f_i^{(l)}(x) = 0$ , and  $\exists \sigma_i^2$  such that  $\mathbb{E} \left[ (f_i^{(l)}(x))^2 \right] < \sigma_i^2 / i^\alpha$ , where the expectation is taken with respect to the prior on the parameters of the neural network; in particular this holds for  $v(x) = f_1^{(n+1)}(x)$ ; this assumption ensures that the prior is well-defined;
7.  $\forall x, y \in [0, 1]^d \exists c_l \geq 0$  such that  $\mathbb{E} \left[ \left( f_i^{(l)}(x) - f_i^{(l)}(y) \right)^2 \right] \leq c_l \|x - y\|^2 / i^\alpha$ , with the expectation again taken with respect to the prior; in particular this gives  $\mathbb{E} [v(x) - v(y)]^2 \leq c_{n+1} \|x - y\|^2$ ; this assumption ensures that the functions one samples behave nicely, and that the output function  $v$  is sufficiently smooth;
8.  $\partial v(x) / \partial x \neq 0$   $\mu_0$ -almost surely, i.e. information from the input layer informs the output layer.

We now state a theorem which shows that the proposed prior satisfies the desired properties of a prior. To this end, we use an activation function<sup>3</sup>  $\varphi : \mathbb{R} \rightarrow \mathbb{R}$  which satisfies the following condition:

<sup>3</sup>As will be clear from the proof of theorem 1, one may use different activation functions at different layers, which will then all have to satisfy this assumption.

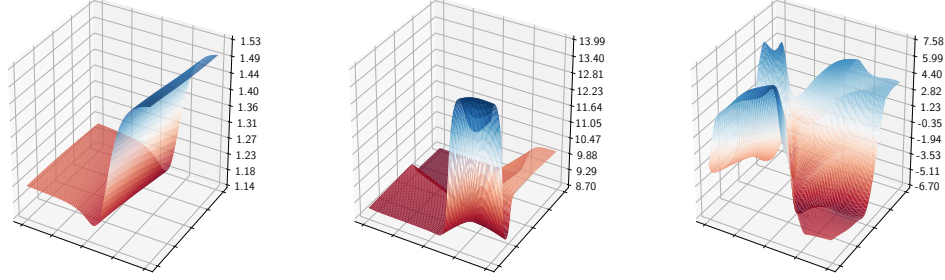


Figure 3: Three samples from the trace-class neural network prior, for a network with 3 fully-connected layers; Tuning parameters are set to  $\alpha = 1.5$ ,  $\sigma_{w^{(l)}}^2 = \sigma_{b^{(l)}}^2 = 2$  for all  $l = 1 \dots n + 1$  (left),  $\alpha = 1.5$ ,  $\sigma_{w^{(l)}}^2 = \sigma_{b^{(l)}}^2 = 20$  (centre),  $\alpha = 1.0001$ ,  $\sigma_{w^{(l)}}^2 = \sigma_{b^{(l)}}^2 = 20$  (right). The tuning parameter  $\alpha$  controls the complexity of the prior functions, the variances in the layers control the overall variance. Note the difference in the magnitudes on the  $z$ -axis.

9.  $\varphi$  is Lipschitz continuous with Lipschitz constant 1 and  $\varphi(0) = 0$ . In particular this implies  $\forall x \in \mathbb{R}$ :  $|\varphi(x)| < |x|$ .<sup>4</sup> Furthermore, this implies that  $\varphi$  is differentiable almost everywhere, with the derivative being essentially bounded by 1.

**Theorem 1.** Under assumption 9, if  $\sigma_{w^{(l)}}^2 > 0$  for all  $l$ , and if the neural network is trace-class (i.e.  $\alpha > 1$ ), the prior satisfies properties 1, 6, 7, and 8.

The proof can be found in Appendix A.2.

### 3.1 Identifiability Issues and Remedies

It is well-known that the output function of a standard neural network does not depend on the labeling of functions within each layer. However, unlike a prior that has uniform variances within each layer, swapping  $f_i^{(l)}$  and  $f_{i+1}^{(l)}$  (effectively by swapping their corresponding weights and biases) will lead from  $\theta$  to a new  $\theta'$  such that  $\mu_0(\theta) \neq \mu_0(\theta')$ , and thus avoid the label-switching problem. To facilitate faster mixing by allowing jumps between these different configurations, we propose Algorithm 1, which can be found in Appendix A.1. The algorithm is in particular useful when using likelihood-informed MCMC algorithms: the likelihood gradients help ‘selecting’ the functions that are important, and then following with a swapping step ensures that they have high prior mass as well. The posterior is invariant with respect to the transition kernel, as the likelihood does not depend on the labelling of the nodes, and as the proposal is symmetric:

$$a(\theta, \theta') = \frac{\mu_0(\theta')}{\mu_0(\theta)} \frac{\mathcal{L}(\theta')}{\mathcal{L}(\theta)} \frac{q(\theta|\theta')}{q(\theta'|\theta)} = \frac{\mu_0(\theta')}{\mu_0(\theta)}. \quad (13)$$

### 3.2 Illustrative Groundwater Flow Example

Before moving on to more challenging examples, we present an illustrative example, and compare the performance of the neural network prior to the Gaussian prior present previously.

#### 3.2.1 Ability to approximate complicated functions

The first aim is to show that the trace-class neural network prior is able to visually recover relatively complicated functions. To this end we define a function  $u^* : [0, 1]^2 \rightarrow \mathbb{R}_+$ , and observe this function on a  $20 \times 20$  grid with independent Gaussian noise  $\mathcal{N}(0, 0.01^2)$ . The true  $u^*$  we used here is the same one as in the example in the next subsection. For the neural network prior we use one hidden layer with 100 nodes, Tanh activation function, and used a four dimensional input space with the inputs  $(x_1, x_2, \sin(x_1), \sin(x_2))$ . We set the tuning parameters to  $\alpha = 1.001$ ,  $\sigma_{w_1}^2 = \sigma_{b_1}^2 = 100$ ,  $\sigma_{w_2}^2 = 1/30$ , and  $\sigma_{b_1}^2 = 1/10$ . As Figure 4 shows, the neural network prior is able to approximate the true  $u^*$  when given many, in this example 400, observations.

<sup>4</sup>The generalisation to arbitrary Lipschitz constants and the implication  $\exists c > 0$  such that  $\forall x \in \mathbb{R}$ :  $|\varphi(x)| < c|x|$  is straightforward.



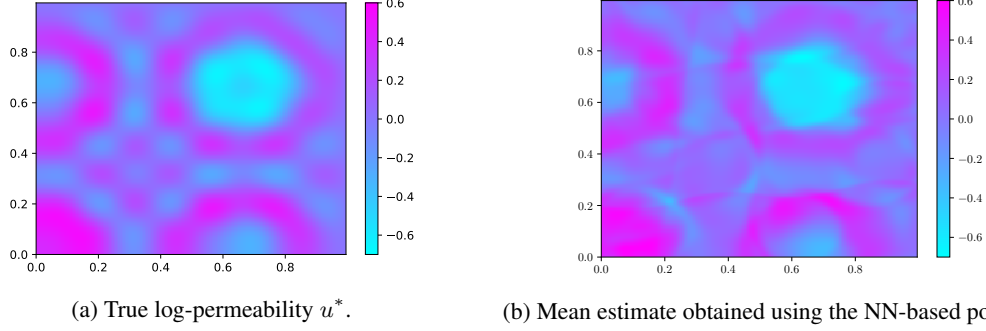


Figure 4: The neural network estimates the true  $u^*(x)$  which is noisily observed on every grid point  $x$  of a  $20 \times 20$  grid. In real applications, only few observations will be available, this example simply illustrates that many observations lead to close approximations for the trace-class neural network prior.

### 3.2.2 Groundwater flow - A Bayesian Inverse Problem

The following example is taken from Beskos et al. [2017]<sup>5</sup>. The aim is to recover the permeability of an aquifer. The following PDE connects the log-permeability  $u$  of a porous medium to the hydraulic head function  $p$ :

$$-\nabla \cdot (\exp(u(x)) \nabla p(x)) = 0 \quad (14)$$

$$p(x) = x_1 \quad \text{if } x_2 = 0 \quad (15)$$

$$p(x) = 1 - x_1 \quad \text{if } x_2 = 1 \quad (16)$$

$$\frac{\partial p(x)}{\partial x_1} = 0 \quad \text{if } x_1 \in \{0, 1\}. \quad (17)$$

To enforce the permeability to be positive, the prior is defined for the log-permeability  $u(x)$ .

We compare two priors. The first one is the trace-class neural network prior described, with the same choice of tuning parameters as before in subsection 3.2.1. The second prior is a Gaussian measure on  $[0, 1]^2$  with the following orthonormal basis and corresponding eigenvalues defined using double indices  $i = (i_1, i_2)$ :

$$\varphi_i(x) = 2 \cos\left(\pi\left(i_1 + \frac{1}{2}\right)x_1\right) \cos\left(\pi\left(i_2 + \frac{1}{2}\right)x_2\right), \quad \lambda_i^2 = \frac{1}{(\pi^2 ((i_1 + 1/2)^2 + (i_2 + 1/2)^2))^{1.1}}. \quad (18)$$

In the experiments, we truncated the basis expansion using  $1 \leq i_1, i_2 \leq 25$ , which gives a similar number of parameters as we used in the neural network example. The true  $u^*$  is now defined using the same basis as  $u^*(x) = \sum_i u_i^* \varphi_i(x)$  with  $u_i^* = \lambda_i \sin((i_1 - 1/2)^2 + (i_2 - 1/2)^2) \cdot \delta[1 \leq i_1, i_2 \leq 10]$ . The data is simulated as a noisy observation of the true hydraulic head function  $p^*$  as obtained by solving the forward PDE on a  $40 \times 40$  grid:  $y = p^*(x) + \varepsilon$ , where  $\varepsilon \sim \mathcal{N}(0, 0.01^2)$ . We ran pCN using both priors, and solving the forward problem on a  $20 \times 20$  grid. Both experiments used a similar number of iterations and stored 1000 MCMC samples to obtain the mean estimates in Figure 5, visual posterior predictive checks are shown in Figure 6.

## 4 Bayesian Reinforcement Learning

In inverse reinforcement learning one aims to learn an agent's value function from observing their series of states and actions. Having the agent's value function at hand allows one to mimic the behaviour of the agent. In a Bayesian approach to this problem, one defines a prior on a function space that includes all admissible value functions. The data observed from an agent's behaviour can then be used through a suitably defined likelihood [Ramachandran and Amir, 2007] to infer the value function.

For discrete state spaces, Singh et al. [2013] provide a method to quantify the uncertainty of the estimated value function. Here, we will generalise those ideas to continuous state spaces by using priors introduced in the previous section.

### 4.1 Setup

A *Markov Decision Process* is defined by a controlled Markov chain  $\{X_n\}_{n \in \mathbb{N}}$  called the *state process*, the *control process*  $\{A_n\}_{n \in \mathbb{N}}$ , and an optimality criterion.

<sup>5</sup>While we could not perfectly replicate their results, we aimed to stick as close to their results as possible.

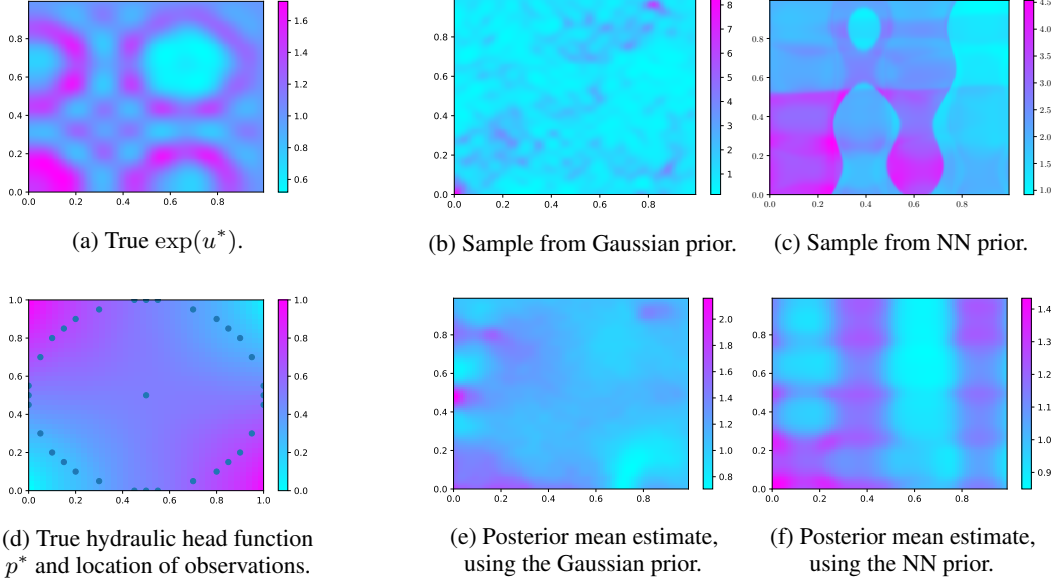


Figure 5: *Left column:* The true log-permeability (a), and its associated hydraulic head function (d) with the location of the 33 observations. *Middle column:* A sample from the Gaussian prior (b), and the posterior mean estimate obtained using pCN for the Gaussian prior (e). *Right column:* A sample from the trace-class neural network prior (c), and the posterior mean estimate obtained using pCN for the neural network prior (f).

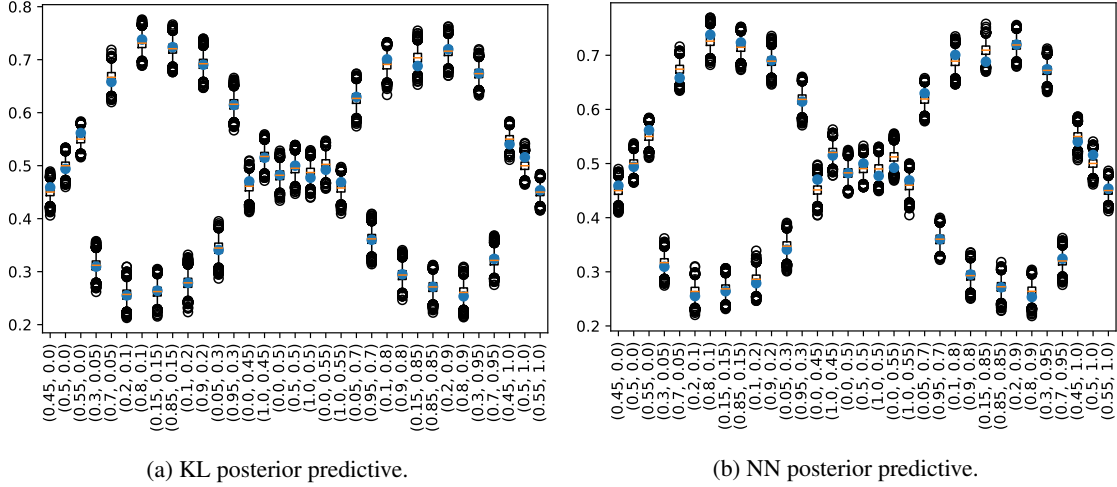


Figure 6: Visual posterior predictive check for both the KL- and NN-based posteriors. The observed values at each of the 33 observation locations (see figure 5) are shown as a blue dot, the box plots are 100 samples from the posterior predictive distribution [Gelman et al., 2013, Section 6.3]. Both posteriors show similar predictive performance indicating that they arise from similarly well-suited priors.

The state process takes values in a bounded set  $\mathcal{X} \subset \mathbb{R}^d$ , for simplicity we will consider the domain to be the  $d$ -dimensional hypercube  $\mathcal{X} = [0, 1]^d$ . The control process is  $\mathcal{A}$ -valued, where  $\mathcal{A} = \{1, \dots, M\}$  is a finite set. Given realisations of the state and actions process until time  $n \geq 0$ , the state process propagates according to

$$X_{n+1} | (X_{1:n} = x_{1:n}, A_{1:n} = a_{1:n}) \sim p(\cdot | x_n, a_n),$$

where for any state-action pair  $(x_n, a_n)$ ,  $p(\cdot | x_n, a_n)$  is a probability density. In some applications, the state dynamics are deterministic, and thus there exists a map  $T$  such that

$$X_{n+1} = T(x_n, a_n). \tag{19}$$

The action process depends on a *policy*  $\mu : \mathcal{X} \rightarrow \mathcal{A}$  which is a deterministic mapping from the state space into the action space:  $A_n | (X_{1:n} = x_{1:n}, A_{1:n-1} = a_{1:n-1}) \sim \delta_{\mu(x_n)}(\cdot)$ .

As there are many possible mappings  $\mu : \mathcal{X} \mapsto \mathcal{A}$ , we assume the agent executes a policy that is in some way optimal. To be more precise, let  $r : \mathcal{X} \rightarrow \mathbb{R}$  be the *reward function*, then the *accumulated reward* given a policy and an initial state  $X_1 = x_1$  is

$$C_\mu(x_1) = \mathbb{E}_\mu \left[ \sum_{n=1}^{\infty} \beta^n r(X_n) | X_1 = x_1 \right],$$

where  $\beta \in (0, 1)$  is a discount factor. The discount factor serves two purposes: it ensures that the expectation is well defined, and also lets early actions be more important than later actions, see Kaelbling et al. [1996] for a more detailed discussion.

A policy  $\mu^*$  is *optimal* if  $C_{\mu^*}(x_1) \geq C_\mu(x_1)$  for all  $(\mu, x_1)$ . The solution to the Bellman equation [Bellman, 1952]

$$v(x) = \max_{a \in \mathcal{A}} \left[ r(x) + \beta \sum_{x' \in \mathcal{X}} p(x'|x, a)v(x') \right]$$

is called the *optimal value function* [Bertsekas, 1995]. Given this fixed point solution  $v$ , we can derive the optimal policy by

$$\mu^*(x) = \arg \max_{a \in \mathcal{A}} \left[ \sum_{x' \in \mathcal{X}} p(x'|x, a)v(x') \right], \quad (20)$$

that is, the optimal action at any state is the one that maximises the expected value function at the next state.

For the observed actions, in what follows we assume the agent is not perfect, e.g. a human expert, and chooses an action with a certain error. At each time step the chosen action is a random variable given by

$$A_n = \arg \max_{a \in \mathcal{A}} \left[ \sum_{x' \in \mathcal{X}} p(x'|x, a)v(x') + \epsilon_n(a) \right], \quad (21)$$

where we assume  $\epsilon_n \sim \mathcal{N}(0, \sigma^2 I_{M \times M})$ . The Gaussian choice simplifies numerical calculations, and it is reasonable to assume that the variances for different actions are independent and identically distributed, but this assumption can be relaxed. When the state dynamics is deterministic, see (19), action selections occur according to

$$A_n = \arg \max_{a \in \mathcal{A}} [v(T(x, a)) + \epsilon_n(a)], \quad (22)$$

Our goal from now on will be to recover the optimal value function, and quantify the uncertainty thereof, by using the Hilbert space MCMC methods and the priors discussed in Sections 2 and 3.

## 4.2 Likelihood definition

The data consists of a collection of state-action pairs  $y = \{y_t\}_{t=1}^T = \{(x_t, a_t)\}_{t=1}^T$  and the aim is to infer the value function (and thus the policy through (20)) that leads to the actions  $a_t$  for the current state  $x_t$ . Using the noisy action selection procedure (21), the likelihood is

$$\mathcal{L}(y|v, \sigma) = \prod_{t=1}^T p(a_t|x_t, v, \sigma) = \prod_{t=1}^T p(a_t|v_t, \sigma), \quad (23)$$

by defining the vector  $v_t$ , containing the relevant evaluations of the value function to calculate the likelihood at  $y_t$ , i.e. using equation (22), the  $k$ -th entry of  $v_t$  is the evaluation of the value function  $v(\cdot)$  at the location  $T(x_t, k)$ , corresponding to starting at  $x_t$  and taking action  $a = k \in \mathcal{A}$ .

For a single observation  $y_t = (x_t, a_t)$ , we now drop the subscript  $t$  to simplify notation, and assume wlog that the optimal action is action  $k = 1$ , permuting the labels if necessary. The probability  $p(a = 1|v, \sigma)$  (where  $v$  is now a vector and  $p(a|v, \sigma)$  is a probability mass function) can be computed using (21) by

$$p(a = 1|v, \sigma) = \int \mathbb{1}_{\{u \in \mathbb{R}^d : u_1 \geq u_j \forall j \neq 1\}} \mathcal{N}(u; v, \sigma^2 I_{M \times M}) du. \quad (24)$$

To compute this term, we make use of the fact that the value of the integral is the same as the probability  $\mathbb{P}(X_1 > X_j, \forall j \neq 1)$ , where  $X_k \sim \mathcal{N}(v(T(x, 1)), \sigma^2)$ . This can be computed numerically using the pdf  $\phi_1(\cdot)$  of  $X_1$  and cdfs  $\Phi_j(\cdot)$  of the respective  $X_j$ :

$$p(a = 1|v, \sigma) = \int_{-\infty}^{\infty} \phi_1(t) \Phi_2(t) \dots \Phi_M(t) dt \quad (25)$$

$$= \frac{1}{\sigma} \int_{-\infty}^{\infty} \phi \left( \frac{t - v_1}{\sigma} \right) \prod_{j=2}^M \Phi \left( \frac{t - v_j}{\sigma} \right) dt. \quad (26)$$

If the noise in (21) is not diagonal, this simplification cannot be made, and the integral (24) is harder to compute. More advanced numerical methods exist to efficiently calculate such integrals using Monte-Carlo simulations [Genz, 1992].

### 4.3 Likelihood gradient

Following from (26) we can compute the gradient of the likelihood in a data point  $(x_t, a_t)$  with respect to  $v_t$ . We again assume wlog that  $a_t = 1 \in \mathcal{A}$  (by permuting the actions if necessary), and drop the subscript  $t$ , emphasising that  $v_k$  is the  $k$ -th entry of the vector  $v$ . The partial derivatives with respect to the  $v_k$  are given by

$$\frac{\partial}{\partial v_1} p(a = 1|v, \sigma) = \frac{1}{\sigma} \int_{-\infty}^{\infty} \frac{t - v_1}{\sigma^2} \phi\left(\frac{t - v_1}{\sigma}\right) \prod_{j=2}^M \Phi\left(\frac{t - v_j}{\sigma}\right) dt \quad (27)$$

$$\frac{\partial}{\partial v_k} p(a = 1|v, \sigma) = -\frac{1}{\sigma^2} \int_{-\infty}^{\infty} \phi\left(\frac{t - v_1}{\sigma}\right) \phi\left(\frac{t - v_k}{\sigma}\right) \prod_{j=2, j \neq k}^M \Phi\left(\frac{t - v_j}{\sigma}\right) dt \quad k = 2 \dots M \quad (28)$$

$$= -\frac{1}{\sigma^2} \phi\left(\frac{v_1 - v_k}{\sqrt{2}\sigma}\right) \int_{-\infty}^{\infty} \phi\left(\frac{t - \frac{v_k + v_1}{2}}{\frac{\sigma}{\sqrt{2}}}\right) \prod_{j=2, j \neq k}^M \Phi\left(\frac{t - v_j}{\sigma}\right) dt, \quad (29)$$

where the last identity follows from the product of two Gaussian pdfs. This allows us, when using the neural network prior, to compute the gradient of the log-likelihood with respect to the parameters of the neural network,  $\theta$ . We emphasise that the vector  $v = v(\theta)$  depends on these parameters, justifying the calculation of the Jacobian  $\mathcal{D}_\theta v$ . Using the chain rule, we get

$$\nabla_\theta \log p(a = 1|v, \sigma) = \frac{\nabla_v p(a = 1|v, \sigma)}{p(a = 1|v, \sigma)} = \frac{(\mathcal{D}_\theta v)^T \nabla_v p(a = 1|v, \sigma)}{p(a = 1|v, \sigma)}. \quad (30)$$

To get the entire gradient of the log-likelihood, we simply need to sum over all data points:

$$\nabla_\theta \ell(y|v, \sigma) = \nabla_\theta \log \left( \prod_{t=1}^T p(a_t|v_t, \sigma) \right) = \nabla_\theta \sum_{t=1}^T \log p(a_t|v_t, \sigma) = \sum_{t=1}^T \nabla_\theta \log p(a_t|v_t, \sigma), \quad (31)$$

where we only need to keep in mind the permutation in the actions when using (30).

When calculating (30), we note that  $1 \cdot \nabla_v p(a|v, \sigma) = 0$  by translation invariance of  $v$ :  $\mathcal{L}(y|v, \sigma) = \mathcal{L}(y|v + c, \sigma)$  for any constant function  $c$ , i.e.  $c(x) = c(x')$  for all  $x, x' \in \mathcal{X}$ . To avoid instabilities when calculating the gradient numerically, we can ensure that the mean of these gradients is 0 by using the following modification, which enhances the performance in practice:

$$(30) = \frac{\sum_{k=1}^M ((\mathcal{D}_\theta v)^T)_k \left( \frac{\partial}{\partial v_k} p(a = 1|v, \sigma) - \sum_{k=1}^M \frac{\partial}{\partial v_k} p(a = 1|v, \sigma) \right)}{p(a = 1|v, \sigma)}. \quad (32)$$

The following theorem justifies the use of this likelihood in the function space MCMC setting:

**Theorem 2.** *The log-likelihood  $\ell(y|v, \sigma) = \log \mathcal{L}(y|v, \sigma)$  defined in (23) satisfies Assumptions 3 and 4, where  $v \in \mathcal{H} = L^2$ .*

The proof can be found in Appendix A.3. We also note that when using the trace-class neural network prior from Section 3, the statements remain true if the likelihood is seen as a function of the parameters  $\theta$  of the neural network:

**Lemma 1.** *The log-likelihood  $\ell(y|v_\theta, \sigma)$  defined in (23) satisfies Assumptions 3 and 4, where now inference is over the weights and biases,  $\theta \in \mathcal{H} = \ell^2$ .*

*Proof.* As  $v$  is a Lipschitz continuous function of  $\theta$ ,  $\ell(y|v(\theta), \sigma)$ , as a composition of Lipschitz continuous functions, is also Lipschitz continuous in  $\theta$ ; and, with an activation function satisfying Condition 9,  $v$  grows at most polynomial in  $\theta$ .  $\square$

The next theorem ensures that the pCNL algorithm is well-defined for both priors by making sure that proposals are  $\mu_0$ -almost surely in the image of the prior:

**Theorem 3.**  *$\mathcal{N}(CD\ell, \mathcal{C}) \simeq \mathcal{N}(0, \mathcal{C})$ , that is, the two Gaussian measures are absolutely continuous with respect to one another. In other words, Condition 5 holds, i.e. the preconditioned gradient of the log-likelihood is in the image of the prior. This holds for both the KL-prior where  $D\ell$  should be understood as the collection of derivatives with respect to the  $\xi_i$  and the prior is over  $\mathcal{H} = L^2$ , and for the trace-class neural network prior, where  $D\ell$  is the collection of derivatives with respect to each weight and bias and inference is over the parameters of the neural network such that  $\mathcal{H} = \ell^2$ .*

The proof can be found in appendix A.4.

## 5 Numerical Illustrations

This section aims to validate the theory, and highlight the applicability of the proposed priors and methodology. In particular, Section 5.2 confirms that, empirically, as the layer width for the trace-class neural network prior grows, the acceptance probability does not go to 0, a property known as ‘stable under mesh-refinement’ or ‘dimension-independence’; Section 5.3 compares the proposed trace-class neural network prior to the Karhunen-Loève prior, and highlights that, unlike the latter, the former is scalable to higher-dimensional domains; and Section 5.4 shows that the posteriors can learn and mimic policies, thus justifying the use of these priors in the reinforcement learning setup.

Throughout we use the Fourier basis (5) as the series expansion of choice when using the Karhunen-Loève based prior, as this proved to be a good choice for reinforcement learning problems [Konidaris et al., 2011]. As a tuning parameter for the corresponding eigenvalues we set  $\alpha = 2$  in (6), forcing the samples to be very smooth which we expect to be a sensible choice in the discussed control problems. For the trace-class neural network prior we used fully connected layers with tanh activation functions throughout. We set the variance parameters uniformly as  $\sigma_{b^{(l)}}^2 = \sigma_{w^{(l)}}^2 = 2$ , and set  $\alpha = 1.5$ , this again results in smooth sample functions.

### 5.1 Control Problems: Setup

We set the scene by describing the setup of the control problems which we use in the experiments.

#### 5.1.1 Mountaincar

The first example is the popular mountaincar problem. The state space is the 2-dimensional domain  $\mathcal{X} = [-1.2, 0.6] \times [-0.07, 0.07]$ , where the first variable is the position  $x_1$  of the car on a mountain slope, and the second variable represents its velocity  $x_2$ . The set of possible actions is  $\mathcal{A} = \{-1, 0, 1\}$ , representing exerting force to the left, not adding force, and exerting force to the right, respectively. The state transitions are deterministic, being given by Newtonian physics, and we refer the reader to the OpenAI documentation or to our code for the details. See Figure 7 for an illustration of the scenario.

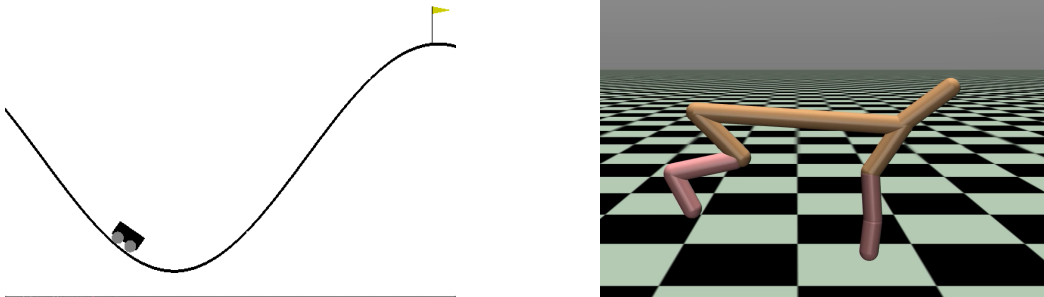


Figure 7: *Left*: The setup for the mountaincar example. The car’s goal is to reach the goal in as few steps as possible. The slope on the right is too steep to simply drive up the mountain, the car therefore has to gain momentum by going up the hill on the left first. *Right*: The HalfCheetah has states  $x_t$  in  $\mathbb{R}^{17}$ . Its goal is to run to the right as quickly as possible, while not moving its body parts more than necessary.

In the mountaincar problem, the reward is constant  $r(x_1, x_2) = -1$  per step, until the car reaches the top of the mountain ( $x_1 \geq 0.5$ ). The optimal policy is therefore to reach the mountaintop as quickly as possible, and we terminate an episode if the car didn’t make it up the hill after 200 time steps. All data was generated from an optimal deterministic policy [Xiao, 2019] given by

$$\mu(x_1, x_2) = -1 + 2\mathbb{I}\{\min(-0.09(x_1 + 0.25)^2 + 0.03, 0.3(x_1 + 0.9)^4 - 0.008) \leq x_2 \leq -0.07(x_1 + 0.38)^2 + 0.07\},$$

and we set the noise level to  $\sigma = 0.1$ .

#### 5.1.2 HalfCheetah

To show that our algorithm works in a more complicated setting, we looked at the HalfCheetah example from the MuJoCo library [Todorov et al., 2012] where the state  $x_t$  a 17-dimensional vector. The original continuous actions space of the problem is 6-dimensional. We discretised the action space to  $M = 20$  actions resulting in a computable likelihood (26), where we set the noise level to  $\sigma = 0.1$ . Positive rewards are given for moving forward, and negative rewards are given for moving backwards. A further penalty is deducted for ‘large’ effort actions, causing the goal to be to move forward as quickly as possible with as little effort as possible.

To generate data, we used as the expert the best performing computed policies from Berkeley’s Deep Reinforcement Learning Course<sup>6</sup>, and projected those actions onto ‘our’ discrete action space by choosing the discrete action minimising the Euclidean distance to the expert’s action.

### 5.2 Dimension independence of trace-class neural network prior under mesh-refinement

We ran pCN for different network widths on the mountaincar example. The Network used has  $l = 3$  hidden layers. As stated before, the tuning parameters in the prior are set to  $\sigma_{b^{(l)}}^2 = \sigma_{w^{(l)}}^2 = 2$ , and  $\alpha = 1.5$ . Table 1 displays the acceptance probability of pCN for fixed step size ( $\beta_{pCN} = 1/10$ ) when targeting the posterior arising from the trace-class neural network prior and the mountaincar likelihood.

$N^{(l)}$ , for all $l$	10	20	30	40	50	60	70	80	90	100
Acc. ratio (in %)	22.8	24.0	23.5	22.1	22.2	23.1	23.9	23.4	23.0	23.9
Total # of param.	261	921	1981	3441	5301	7561	10221	13281	16741	20601

Table 1: Acceptance ratios and total number of parameters (weights and biases) for different layer widths. 3 fully connected layers were used, and pCN was run over 3 hours for each of the layer widths. Notably the acceptance probability does not degenerate as more nodes are included per layer.

### 5.3 Comparison of priors

To compare the trace-class neural network prior to the Karhunen-Loève prior, we used a large number of parameters for each, such that the error from truncating after finitely many nodes, or finitely many terms, is negligible. For both the mountaincar and the HalfCheetah example, we used the same trace-class neural network prior, with 3 hidden layers, and 100 nodes per layer, resulting in 20,601 parameters to be estimated for the mountaincar example, and 22,101 for the HalfCheetah example. For the Karhunen-Loève prior in the mountaincar example we set the truncation parameter to  $k_{max} = 70$  for (5) with eigenvalues (6) (recall that here  $\alpha = 2$ ), resulting in a total of 19,880 coefficients to be estimated. For the KL prior in the HalfCheetah example we used approximation (3), and otherwise the same eigenfunctions and eigenvalues; due to the higher domain dimension  $d = 17$ , one would have to estimate 2,667,980 parameters. As this is too memory-expensive for the computer used for the experiments, we used  $k_{max} = 10$  in the HalfCheetah example, resulting in 54,740 parameters to be estimated. Note that this increase in parameters to be estimated is already due to the approximation (3) being used, and additionally truncating the expansions after fewer terms, highlighting the benefits of the dimension-robustness of the trace-class neural network prior.

To assess the quality of the priors, we ran pCN using 50 (for the mountaincar) and 100 (for the HalfCheetah) data points. For the mountaincar example, we fixed five test points  $z_j, j = 1, \dots, 5$ , and compared the posteriors by evaluating  $v(z_j)$  at these new locations as estimated through MCMC runs. The top row in Figure 8 shows the resulting uncertainty estimates. As the value function is invariant under translations, we adjusted all samples such that they take the value 0 at the state which the optimal action takes one to.

For the HalfCheetah example, we looked at one test point for illustration, see the bottom row in Figure 8, and summarised the performance on another 100 data points in the Table 2, where we compared how the respective samples from the posterior do, as well as how the mean of all samples from the posterior in Section 5.4 (with a smaller number of nodes for the NN prior, and fewer active terms in the KL prior<sup>7</sup>) does on predicting the correct action (last two columns). Not surprisingly, the mean function is better at picking the correct action.

### 5.4 Ability to Learn Policy

To assess if the posteriors can truly learn an agent’s behaviour, we used the priors with a smaller number of parameters, and stored 1000 samples for each posterior. We then used these samples to obtain a mean value function which was

<sup>6</sup>CS294-112 HW 1: Imitation Learning, <https://github.com/berkeleydeeprlcourse/homework/tree/master/hw1>, accessed on December 4th, 2020.

<sup>7</sup>To calculate the mean function it is necessary to store the samples which (due to their used computer’s limited memory capacity) would not be feasible for the very wide layer prior, nor all the terms in the KL prior.

Decision made by	KL samples	NN samples	KL mean	NN mean
Optimal Action	20.1%	32.1%	25%	42%
Non-optimal Action	79.9%	67.9%	75%	58%

Table 2: Optimal action picked by samples, and the sample mean at a data point, for two different posteriors. The trace-class neural network prior outperforms the approximate KL prior.

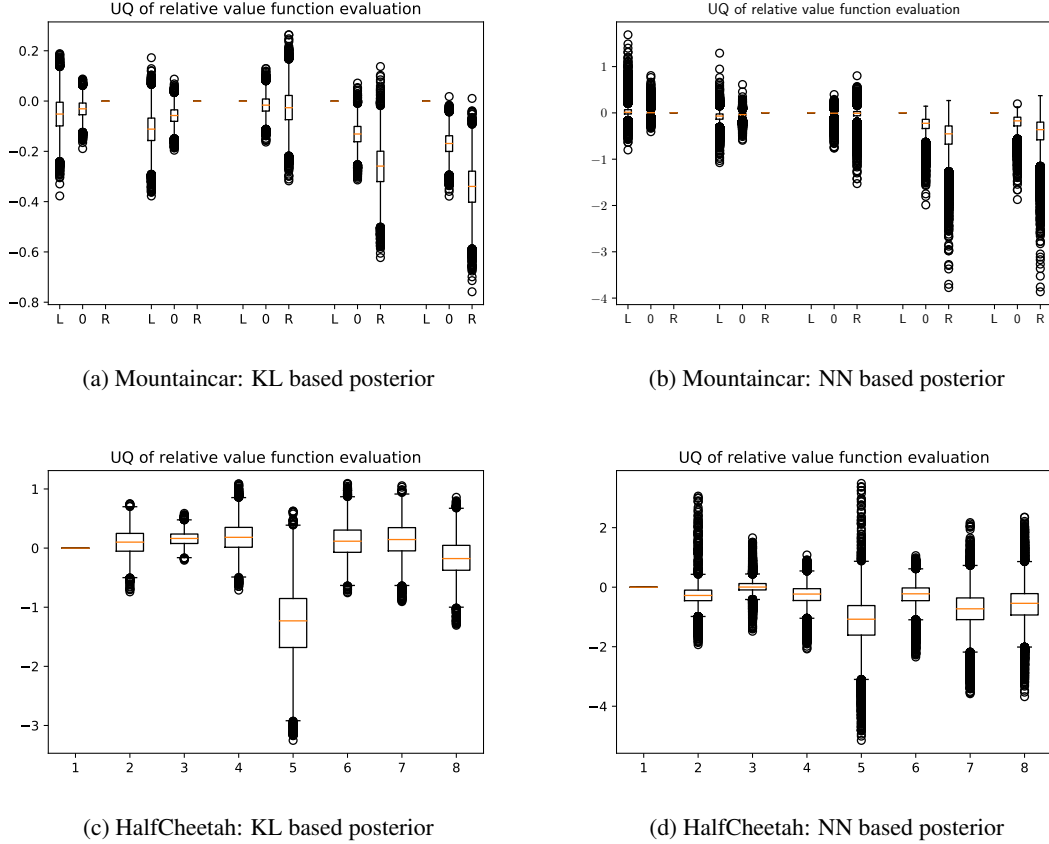


Figure 8: Uncertainty estimates arising from the two different priors for the mountaincar and the HalfCheetah examples. *Top row:* Mountaincar example. In each plot, five different states are looked at, the estimates of the value functions are shown, standardised such that the optimal action has value 0 always. Both the Karhunen-Lo eve based posterior and the neural network based posterior can make no clear judgement as to what the optimal actions for the first three shown states are. For the fourth and fifth states, both posteriors suggest a clear decision for action ‘Left’. The reader should note that both the KL and the NN posteriors behave similarly in that they are uncertain in the first three states, and very decisive in the last two states. *Bottom row:* HalfCheetah example. The optimal action is the first one in both plots, and samples are normalised such that they take the value 0 at the state the optimal value takes one to. The NN posterior correctly estimates the optimal action, the KL posterior doesn’t.

used for decision making. For the trace-class neural network prior we used 3 layers with 10 nodes per layer for both examples (resulting in 261 parameters for the mountaincar example and 411 for the HalfCheetah); for the KL prior we used  $k_{max} = 7$  for the mountaincar example (giving a total of 224 parameters), and  $k_{max} = 5$  in the HalfCheetah example (a total of 8,730 parameters). The results are summarised in Figure 9.

## 6 Conclusion and Outlook

This paper addresses the problem of effective Bayesian inference for unknown functions with higher dimensional domains. Unlike priors which require an orthogonal basis for the function space, and scales exponentially in the domain dimension, our proposed trace-class neural network prior easily scales to higher-dimensional domains as the dependence on the domain dimension is linear. When using the pCN sampling method, this prior also satisfies the desired property of being stable under mesh-refinement, in the sense that the acceptance probability of pCN does not degenerate to 0 when using more parameters for the neural network. Various questions remain unanswered though, and interesting directions of research open up: are there suitable further generalisations of the proposed prior, e.g. heavy-tailed or hierarchical ones, which still satisfy the desired properties, enabling the use of these priors in the function space setting? What are the optimal settings for the tuning parameters  $\sigma_w^{2(l)}$ ,  $\sigma_b^{2(l)}$  and  $\alpha$ ? Can one obtain contraction rates to ensure the concentration of the posterior samples around the true functions? A first idea here is to exploit the various

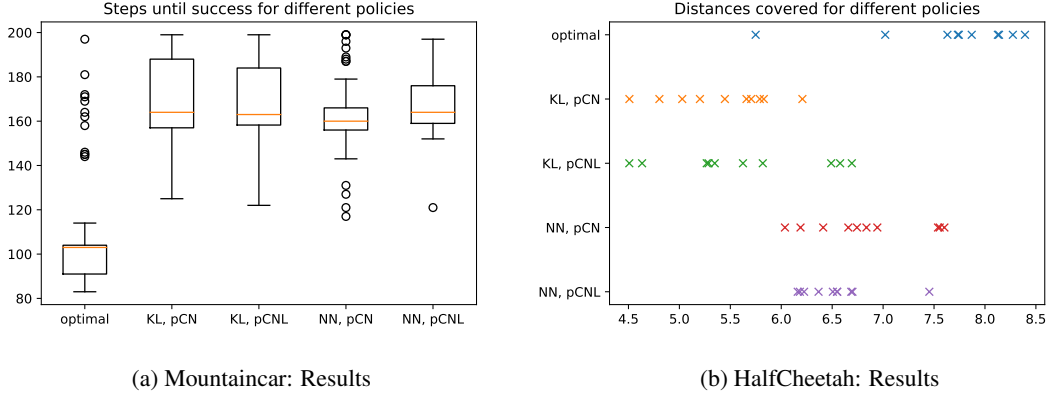


Figure 9: Results for the policy learning experiment.

*Left:* Mountaincar example. The number of steps until success is shown for different posteriors. If the goal was not reached after 200 steps, the run was counted as failure. Out of 100 runs, the policy following the KL posterior when using pCN gave 34 failures (24 when using pCNL), the NN posteriors gave 23 (for the posterior estimates obtained using pCN) and 25 (pCNL).

*Right:* HalfCheetah example. The different policies arising from the KL posterior (obtained once using pCN, once using pCNL) and the NN posterior were controlling the agent over 10 runs with 100 time steps. The distances covered per run are shown in the plot.

generalisations of the universal approximation theorem, and combine them with the proof methodology used in this paper.

We further introduced a likelihood suitable for Bayesian reinforcement learning where the underlying Markov decision process has a continuous state-space, and thus the unknown value function to be estimated has domain  $\mathbb{R}^d$  as opposed to a discrete set. An interesting research direction is to generalise this to continuous action spaces as well.

Finally, we underscored the theory with numerical illustrations, illustrating the applicability of the prior in various control problems.

## References

- Sergios Agapiou, Stig Larsson, and Andrew M Stuart. Posterior contraction rates for the bayesian approach to linear ill-posed inverse problems. *Stochastic Processes and their Applications*, 123(10):3828–3860, 2013.
- Krishna B Athreya and Peter Ney. A new approach to the limit theory of recurrent markov chains. *Transactions of the American Mathematical Society*, 245:493–501, 1978.
- Richard Bellman. On the theory of dynamic programming. *Proceedings of the National Academy of Sciences of the United States of America*, 38(8):716, 1952.
- Dimitri P Bertsekas. *Dynamic programming and optimal control*, volume 1. Athena scientific Belmont, MA, 1995.
- Alexandros Beskos, Gareth Roberts, Andrew Stuart, and Jochen Voss. Mcmc methods for diffusion bridges. *Stochastics and Dynamics*, 8(03):319–350, 2008.
- Alexandros Beskos, Mark Girolami, Shiwei Lan, Patrick E Farrell, and Andrew M Stuart. Geometric mcmc for infinite-dimensional inverse problems. *Journal of Computational Physics*, 335:327–351, 2017.
- Steve Brooks, Andrew Gelman, Galin Jones, and Xiao-Li Meng. *Handbook of markov chain monte carlo*. CRC press, 2011.
- Robert H Cameron and William T Martin. Transformations of weiner integrals under translations. *Annals of Mathematics*, pages 386–396, 1944.
- Simon L Cotter, Gareth O Roberts, Andrew M Stuart, and David White. Mcmc methods for functions: modifying old algorithms to make them faster. *Statistical Science*, pages 424–446, 2013.
- Tiangang Cui, Kody JH Law, and Youssef M Marzouk. Dimension-independent likelihood-informed mcmc. *Journal of Computational Physics*, 304:109–137, 2016.
- Giuseppe Da Prato and Jerzy Zabczyk. *Stochastic equations in infinite dimensions*. Cambridge university press, 2014.



- Andreas Damianou and Neil Lawrence. Deep gaussian processes. In *Artificial Intelligence and Statistics*, pages 207–215, 2013.
- Masoumeh Dashti, Stephen Harris, and Andrew Stuart. Besov priors for bayesian inverse problems. *arXiv preprint arXiv:1105.0889*, 2011.
- Masoumeh Dashti, Kody JH Law, Andrew M Stuart, and Jochen Voss. Map estimators and their consistency in bayesian nonparametric inverse problems. *Inverse Problems*, 29(9):095017, 2013.
- Matthew M Dunlop, Mark A Girolami, Andrew M Stuart, and Aretha L Teckentrup. How deep are deep gaussian processes? *The Journal of Machine Learning Research*, 19(1):2100–2145, 2018.
- Andreas Eberle et al. Error bounds for metropolis–hastings algorithms applied to perturbations of gaussian measures in high dimensions. *The Annals of Applied Probability*, 24(1):337–377, 2014.
- Andrew Gelman, John B Carlin, Hal S Stern, David B Dunson, Aki Vehtari, and Donald B Rubin. *Bayesian data analysis*. CRC press, 2013.
- Alan Genz. Numerical computation of multivariate normal probabilities. *Journal of computational and graphical statistics*, 1(2):141–149, 1992.
- Evarist Giné and Richard Nickl. *Mathematical foundations of infinite-dimensional statistical models*, volume 40. Cambridge University Press, 2016.
- Martin Hairer, Andrew M Stuart, Sebastian J Vollmer, et al. Spectral gaps for a metropolis–hastings algorithm in infinite dimensions. *The Annals of Applied Probability*, 24(6):2455–2490, 2014.
- Enkelejd Hashorva. Asymptotics and bounds for multivariate gaussian tails. *Journal of theoretical probability*, 18(1): 79–97, 2005.
- W Keith Hastings. Monte carlo sampling methods using markov chains and their applications. 1970.
- Kurt Hornik. Approximation capabilities of multilayer feedforward networks. *Neural networks*, 4(2):251–257, 1991.
- Bamdad Hosseini. Well-posed bayesian inverse problems with infinitely divisible and heavy-tailed prior measures. *SIAM/ASA Journal on Uncertainty Quantification*, 5(1):1024–1060, 2017.
- Bamdad Hosseini and Nilima Nigam. Well-posed bayesian inverse problems: Priors with exponential tails. *SIAM/ASA Journal on Uncertainty Quantification*, 5(1):436–465, 2017.
- Marco A Iglesias, Kody JH Law, and Andrew M Stuart. Evaluation of gaussian approximations for data assimilation in reservoir models. *Computational Geosciences*, 17(5):851–885, 2013.
- Arieh Iserles and Syvert P Nørsett. From high oscillation to rapid approximation iii: Multivariate expansions. *IMA journal of numerical analysis*, 29(4):882–916, 2009.
- Leslie Pack Kaelbling, Michael L Littman, and Andrew W Moore. Reinforcement learning: A survey. *Journal of artificial intelligence research*, 4:237–285, 1996.
- Bartek T Knapik, Aad W Van Der Vaart, J Harry van Zanten, et al. Bayesian inverse problems with gaussian priors. *The Annals of Statistics*, 39(5):2626–2657, 2011.
- George Konidaris, Sarah Osentoski, and Philip Thomas. Value function approximation in reinforcement learning using the fourier basis. In *Twenty-fifth AAAI conference on artificial intelligence*, 2011.
- Benedict Leimkuhler, Charles Matthews, and Tiffany Vlaar. Partitioned integrators for thermodynamic parameterization of neural networks. *arXiv preprint arXiv:1908.11843*, 2019.
- Zachary C Lipton. The mythos of model interpretability. *Queue*, 16(3):31–57, 2018.
- Alexander G de G Matthews, Mark Rowland, Jiri Hron, Richard E Turner, and Zoubin Ghahramani. Gaussian process behaviour in wide deep neural networks. *arXiv preprint arXiv:1804.11271*, 2018.
- Brent Minchew, Mark Simons, Scott Hensley, Helgi Björnsson, and Finnur Pálsson. Early melt season velocity fields of langjökull and hofsjökull, central iceland. *Journal of Glaciology*, 61(226):253–266, 2015.
- Radford M Neal. *Bayesian learning for neural networks*, volume 118. Springer Science & Business Media, 2012.
- RM Neal. Bayesian learning for neural networks [phd thesis]. *Toronto, Ontario, Canada: Department of Computer Science, University of Toronto*, 1995.
- RM Neal. Regression and classification using gaussian process priors. *Bayesian statistics*, 6:475, 1998.
- Richard Nickl and Matteo Giordano. Consistency of bayesian inference with gaussian process priors in an elliptic inverse problem. *Inverse Problems*, 2020.

- ALFIO Quarteroni, Andrea Manzoni, and Christian Vergara. The cardiovascular system: mathematical modelling, numerical algorithms and clinical applications. *Acta Numerica*, 26:365–590, 2017.
- Deepak Ramachandran and Eyal Amir. Bayesian inverse reinforcement learning. In *IJCAI*, volume 7, pages 2586–2591, 2007.
- Gareth O Roberts and Jeffrey S Rosenthal. Optimal scaling of discrete approximations to langevin diffusions. *Journal of the Royal Statistical Society: Series B (Statistical Methodology)*, 60(1):255–268, 1998.
- Gareth O Roberts, Richard L Tweedie, et al. Exponential convergence of langevin distributions and their discrete approximations. *Bernoulli*, 2(4):341–363, 1996.
- Gareth O Roberts, Jeffrey S Rosenthal, et al. Optimal scaling for various metropolis-hastings algorithms. *Statistical science*, 16(4):351–367, 2001.
- Daniel Rudolf and Björn Sprungk. On a generalization of the preconditioned crank–nicolson metropolis algorithm. *Foundations of Computational Mathematics*, 18(2):309–343, 2018.
- I Richard Savage. Mills’ ratio for multivariate normal distributions. *J. Res. Nat. Bur. Standards Sect. B*, 66:93–96, 1962.
- Sumeetpal S Singh, Nicolas Chopin, and Nick Whiteley. Bayesian learning of noisy markov decision processes. *ACM Transactions on Modeling and Computer Simulation (TOMACS)*, 23(1):4, 2013.
- Ilya M Sobol. Sensitivity estimates for nonlinear mathematical models. *Mathematical modelling and computational experiments*, 1(4):407–414, 1993.
- Andrew M Stuart. Inverse problems: a bayesian perspective. *Acta numerica*, 19:451–559, 2010.
- Luke Tierney et al. A note on metropolis-hastings kernels for general state spaces. *The Annals of Applied Probability*, 8(1):1–9, 1998.
- Emanuel Todorov, Tom Erez, and Yuval Tassa. Mujoco: A physics engine for model-based control. In *2012 IEEE/RSJ International Conference on Intelligent Robots and Systems*, pages 5026–5033. IEEE, 2012.
- Aad W van der Vaart, J Harry van Zanten, et al. Rates of contraction of posterior distributions based on gaussian process priors. *The Annals of Statistics*, 36(3):1435–1463, 2008.
- Max Welling and Yee W Teh. Bayesian learning via stochastic gradient langevin dynamics. In *Proceedings of the 28th international conference on machine learning (ICML-11)*, pages 681–688, 2011.
- Florian Wenzel, Kevin Roth, Bastiaan S Veeling, Jakub Świątkowski, Linh Tran, Stephan Mandt, Jasper Snoek, Tim Salimans, Rodolphe Jenatton, and Sebastian Nowozin. How good is the bayes posterior in deep neural networks really? *arXiv preprint arXiv:2002.02405*, 2020.
- Przemyslaw Wojtaszczyk. *A mathematical introduction to wavelets*, volume 37. Cambridge University Press, 1997.
- Zhiqing Xiao. *Reinforcement Learning: Theory and Python Implementation*. China Machine Press, 2019.

## A Appendix

### A.1 NodeSwap Algorithm

---

**Algorithm 1**


---

```

1: procedure NODESWAP( $\theta$ ) ▷ Input current iterate  $\theta$ 
2:    $\theta' \leftarrow \theta$ 
3:    $l \sim Unif(n)$  ▷ Sample random layer
4:    $i \sim Geom(\alpha^{-1})$  ▷ Sample random node
5:   while  $i \geq N_l$  do ▷ Repeat process until we have a valid node index
6:      $i \sim Geom(\alpha^{-1})$ 
7:   end while
8:    $w_{i+1,j}^{(l)'} \leftarrow w_{i,j}^{(l)}$ 
9:    $w_{i,j}^{(l)'} \leftarrow w_{i+1,j}^{(l)}$ 
10:   $w_{i,j+1}^{(l+1)'} \leftarrow w_{i,j}^{(l+1)}$ 
11:   $w_{i,j}^{(l+1)'} \leftarrow w_{i,j+1}^{(l+1)}$ 
12:   $b_{i+1}^{(l)'} \leftarrow b_i^{(l)}$ 
13:   $b_i^{(l)'} \leftarrow b_{i+1}^{(l)}$ 
14:   $u \sim Unif([0, 1])$ 
15:   $a = \min(1, \mu_0(\theta')/\mu_0(\theta))$  ▷ Metropolis-Hastings acceptance probability cf. (13)
16:  if  $u < a$  then
17:    return  $\theta'$  ▷ Accept node swap
18:  else
19:    return  $\theta$  ▷ Reject node swap
20:  end if
21: end procedure

```

---

### A.2 Proof of Theorem 1

*Proof of Theorem 1.* We firstly show assumption 1: Let the Hilbert space  $\mathcal{H}$  be the set

$$\mathcal{H} = \left\{ \theta = (w, b) : \sum_{l=1}^{n+1} \sum_{i=1}^{\infty} \left( (b_i^{(l)})^2 + \sum_{j=1}^{\infty} (w_{i,j}^{(l)})^2 \right) < \infty \right\} \quad (33)$$

equipped with the inner product

$$\langle \theta, \tau \rangle = \langle (w, b), (\varpi, \beta) \rangle = \sum_{l=1}^{n+1} \sum_{i=1}^{\infty} \left( b_i^{(l)} \beta_i^{(l)} + \sum_{j=1}^{\infty} w_{i,j}^{(l)} \varpi_{i,j}^{(l)} \right).$$

This Hilbert space can be interpreted as the  $l^2$  sequence space, and equivalently as the direct sum of countably many  $l^2$  sequence spaces  $\mathcal{H}_i^{(l)} = \{(w_i^{(l)}, b_i^{(l)}) : (b_i^{(l)})^2 + \sum_{j=1}^{\infty} (w_{i,j}^{(l)})^2 < \infty\}$ .

We now show that any sample from the prior (11) is in this Hilbert space almost surely. To see this, we define the random variables

$$S_k^{(l)} = \sum_{i=1}^k \left( (B_i^{(l)}) + \sum_{j=1}^k (W_{i,j}^{(l)}) \right). \quad (34)$$

It's easy to check that  $S_k^{(l)}$  is a  $L^2$ -bounded martingale if  $\sum_{i=1}^{\infty} \mathbb{E} \left[ (B_i^{(l)})^2 \right] < \infty$  and  $\sum_{i,j=1}^{\infty} \mathbb{E} \left[ (W_{i,j}^{(l)})^2 \right] < \infty$ , which is the case for our choice of the prior, as long as  $\alpha > 1$ . Therefore  $S_k^{(l)}$  converges almost surely to some limit  $S^{(l)}$  by the  $L^2$ -martingale convergence theorem, so  $S^{(l)} \in \mathcal{H}$  as required.

To see the second part of assumption 1, note that the sequences  $e_1, e_2, \dots$  form a basis of  $l^2$ , and therefore of  $\mathcal{H}$ , and the summability of the variances (given if  $\alpha > 1$ ) ensures that the prior covariance operator is indeed trace-class.

To see Assumption 6, by looking at the first layer we can easily check that for fixed  $x \in [0, 1]^d$ ,  $f_i^{(1)}(x)$  is a mixture of centered Gaussian distributions, and the claim follows by noting that  $\mathbb{E}B_i^{(1)} = \mathbb{E}W_{i,j}^{(1)} = 0$ ,

$$\begin{aligned} \mathbb{E} \left[ (f_i^{(1)}(x))^2 \right] &= \mathbb{E} \left[ (B_i^{(1)})^2 \right] + \sum_{j=1}^d \mathbb{E} \left[ (W_{i,j}^{(1)})^2 \right] (x_j)^2 \\ &\leq \frac{\sigma_{b_1}^2}{i^\alpha} + \frac{\sigma_{w_1}^2}{i^\alpha} d \end{aligned} \quad (35)$$

$$= \frac{1}{i^\alpha} [\sigma_{b_1}^2 + \sigma_{w_1}^2 d]. \quad (36)$$

We use induction over  $l$ , and define the following random variables, for which we truncate the  $i$ -th function of layer  $l$  after  $k$  terms:

$$f_{i,k}^{(l)}(x) = B_i^{(l)} + \sum_{j=1}^k W_{i,j}^{(l)} \varphi(f_j^{(l-1)}(x)) \quad l = 2 \dots n+1.$$

It will be useful to note that by Assumption 9 and the induction hypothesis, we get

$$|\varphi(f_j^{(l-1)}(x))| \leq |(f_j^{(l-1)}(x))| < \infty. \quad (37)$$

Furthermore, from the above and using Jensen's inequality, we also obtain

$$|\mathbb{E}\varphi(f_j^{(l-1)}(x))| \leq \mathbb{E}[|\varphi(f_j^{(l-1)}(x))|] \leq \mathbb{E}[|f_j^{(l-1)}(x)|] < \infty, \quad (38)$$

where the last inequality holds as  $f_j^{(l-1)}(x)$  is  $L^2$  bounded by the induction hypothesis.

We now show that  $f_{i,k}^{(l)}(x) \rightarrow f_i^{(l)}(x)$  almost surely, and in  $L^2$ , by applying the  $L^2$  martingale convergence theorem.

We thus need to show that  $S_k(x) := f_{i,k}^{(l)}(x)$  is a  $L^2$  bounded martingale, where we dropped the indices  $i$  and  $l$  for notational convenience. Indeed, with the natural filtration  $(\mathcal{F}_k)_{k \in \mathbb{N}}$

$$\mathbb{E}[S_{k+1}(x)|\mathcal{F}_k] = 0,$$

as  $W_{i,j}^{(l)}$  and  $\varphi(f_j^{(l-1)}(x))$  are independent, the expectation of the former is centered, and the latter is finite. Additionally, by exploiting the independence, Assumption 9 and 38, we get

$$\mathbb{E} \left[ (S_k(x))^2 \right] = \mathbb{E}[B_i^{(l)}]^2 + \sum_{j=1}^k \mathbb{E} \left[ (W_{i,j}^{(l)})^2 \right] \mathbb{E} \left[ (\varphi(f_j^{(l-1)}(x)))^2 \right] \quad (39)$$

$$\begin{aligned} &\leq \frac{\sigma_{b^{(l)}}^2}{i^\alpha} + \sigma_{w^{(l)}}^2 \sum_{j=1}^k \frac{1}{(ij)^\alpha} \mathbb{E} \left[ (f_j^{(l-1)}(x))^2 \right] \\ &\leq \frac{\sigma_{b^{(l)}}^2}{i^\alpha} + \frac{\sigma_{w^{(l)}}^2 \sigma_{l-1}^2}{i^\alpha} \sum_{j=1}^k \frac{1}{j^{2\alpha}} \end{aligned} \quad (40)$$

$$= \frac{1}{i^\alpha} \left[ \sigma_{b^{(l)}}^2 + \sigma_{w^{(l)}}^2 \sigma_{l-1}^2 \sum_{j=1}^k \frac{1}{j^{2\alpha}} \right]. \quad (41)$$

This series converges for  $\alpha > 1$ , and we define the limit for  $i = 1$  as  $\sigma_l^2$ . Thus,  $S_k$  is indeed a  $L^2$  bounded martingale and trivially  $\mathbb{E}f_i^{(l)} = 0$ , proving Assumption 6.

It remains to show 7. For the first layer, we use independence to get

$$\begin{aligned} \mathbb{E} \left[ (f_i^{(1)}(x) - f_i^{(1)}(y))^2 \right] &= \sum_{j=1}^d \mathbb{E} \left[ (W_{i,j}^{(1)})^2 \right] (x_j - y_j)^2 \\ &= \frac{\sigma_{w_1}^2}{i^\alpha} \|x - y\|^2. \end{aligned} \quad (42)$$

For the subsequent layers, we again use induction over  $l$ . We define  $S_k(x)$  as before and check that

$$\mathbb{E} [(S_k(x)S_k(y))^2] = \mathbb{E} [(B_i^{(l)})^2] + \sum_{j=1}^k \mathbb{E} [(W_{i,j}^{(l)})^2] \mathbb{E} [\varphi(F_j^{(l-1)}(x))\varphi(F_j^{(l-1)}(y))]. \quad (43)$$

Using the induction hypothesis, Assumption 9, (39) and (43) we get

$$\begin{aligned} \mathbb{E} [(S_k(x) - S_k(y))^2] &= \mathbb{E} [(S_k(x))^2] + \mathbb{E} [(S_k(y))^2] - 2\mathbb{E}[S_k(x)S_k(y)] \\ &= 2\mathbb{E} [(B_i^{(l)})^2] + \sum_{j=1}^k \mathbb{E} [(W_{i,j}^{(l)})^2] \left( \mathbb{E} [\varphi(F_j^{(l-1)}(x))^2] + \mathbb{E} [\varphi(F_j^{(l-1)}(y))^2] \right) - 2\mathbb{E}[S_k(x)S_k(y)] \\ &= \sigma_{w^{(l)}}^2 \sum_{j=1}^k \frac{1}{(ij)^\alpha} \mathbb{E} [(\varphi(F_j^{(l-1)}(x)) - \varphi(F_j^{(l-1)}(y)))^2] \\ &\leq \sigma_{w^{(l)}}^2 \sum_{j=1}^k \frac{1}{(ij)^\alpha} \mathbb{E} [(f_j^{(l-1)}(x) - f_j^{(l-1)}(y))^2] \\ &\leq \frac{\sigma_{w^{(l)}}^2 c_{l-1}}{i^\alpha} \|x - y\|^2 \sum_{j=1}^k \frac{1}{j^{2\alpha}} \end{aligned} \quad (44)$$

$$= \frac{1}{i^\alpha} \left[ \sigma_{w^{(l)}}^2 c_{l-1} \sum_{j=1}^k \frac{1}{j^{2\alpha}} \right] \|x - y\|^2, \quad (45)$$

such that the claim follows upon defining  $c_l = \sigma_{w^{(l)}}^2 c_{l-1} \sum_{j=1}^\infty 1/j^{2\alpha}$ .

Lastly, Property 8 follows immediately, as the property is only violated if all weights are 0, which is a zero probability event as long as  $\sigma_{w^{(l)}}^2 > 0$ .  $\square$

### A.3 Proof of Theorem 2

*Proof of Theorem 2.* In the following, we identify  $v$  with its finitely many observations  $v_t$ . One notes that the integral (24) is upper bounded by 1. For the lower bound we substitute  $w = u - v$  in (24), allowing us to bound

$$\begin{aligned} (24) &= \int \mathbb{1}_{\{u \in \mathbb{R}^d: (w+v)_1 \geq (w+v)_j \forall j \neq 1\}} \mathcal{N}(w; 0, \sigma^2 I_{M \times M}) dw \\ &\geq \int \mathbb{1}_{\{w \in \mathbb{R}^d: (w+v)_1 \geq 0 \geq (w+v)_j \forall j \neq 1\}} \mathcal{N}(w; 0, \sigma^2 I_{M \times M}) dw \\ &= \int \mathbb{1}_{\{w \in \mathbb{R}^d: w_1 \geq -v_1, w_j \leq -v_j \forall j \neq 1\}} \mathcal{N}(w; 0, \sigma^2 I_{M \times M}) dw \\ &= \int \mathbb{1}_{\{w \in \mathbb{R}^d: w_1 \geq -v_1, w_j \geq v_j \forall j \neq 1\}} \mathcal{N}(w; 0, \sigma^2 I_{M \times M}) dw \end{aligned} \quad (46)$$

$$\begin{aligned} &\geq \int \mathbb{1}_{\{w \in \mathbb{R}^d: w_1 \geq |-v_1|, w_j \geq |v_j| \forall j \neq 1\}} \mathcal{N}(w; 0, \sigma^2 I_{M \times M}) dw \\ &\geq \int \mathbb{1}_{\{w \in \mathbb{R}^d: w_1 \geq s, w_j \geq s \forall j \neq 1\}} \mathcal{N}(w; 0, \sigma^2 I_{M \times M}) dw, \end{aligned} \quad (47)$$

where for (46) we exploited the fact that the normal is centered and isotropic, and to get (47) we pick  $s = \|v\|_\infty > 0$  if  $v \neq 0$ . The case  $v = 0$  is trivial as the integral is then non-zero. (47) can now be treated as the tail probability for a centered multivariate normal distribution (see Hashorva [2005]) which satisfies the Savage condition Savage [1962]. We thus get the bound

$$(47) \geq c \exp(-s^2) = c \exp(-\|v\|_\infty^2)$$

as long as  $\|v\|_\infty > 2d/\sigma^4$ . For all other  $v$ , the integral (24) is bounded away from zero, and the Assumption 3 holds trivially. The assumption thus holds for all  $v$ .

To see that Assumption 4 holds, note that the log-likelihood is continuously differentiable in  $v$ , and thus locally Lipschitz.  $\square$

#### A.4 Proof of Theorem 3

*Proof of Theorem 3.* Firstly, note that the Assumptions in Theorem 1 hold by Theorem 2, and additionally the log-likelihood  $\ell$  satisfies  $\sum_{k=1}^M \frac{\partial \ell}{\partial v_k} = 0$  (where  $v_k$  is the evaluation  $v(x_k)$  of the value function at location  $x_k$ ) by the translation invariance, and  $\sum_{k=1}^M \left(\frac{\partial \ell}{\partial v_k}\right)^2 < \infty$  for any  $v$   $\mu_0$ -almost surely.

For the KL prior, the claim follows immediately from the Feldman-Hajek theorem (see e.g. Da Prato and Zabczyk [2014])

For simplicity, we from now on assume that the likelihood consists of only one data point and omit the respective index, but the generalisation to multiple data points is trivial.

Following a similar argument as in the proof of Theorem 1, we want to show that

$$S_s = \sum_{l=1}^{n+1} \sum_{i=1}^s \left[ \left( \frac{\partial \ell}{\partial B_i^{(l)}} \right) + \sum_{j=1}^s \left( \frac{\partial \ell}{\partial W_{i,j}^{(l)}} \right) \right] \quad (48)$$

defines a  $L^2$ -bounded martingale, converging almost surely by the  $L^2$  martingale convergence theorem.

Once we have established the convergence, we note that this implies the equivalence  $\mathcal{N}(\mathcal{CD}\ell, \mathcal{C}) \simeq \mathcal{N}(0, \mathcal{C})$  by applying the Feldman-Hajek theorem. We here also note that, if we want to apply the same argument for the case without preconditioning, we would require

$$\mathbb{E}[(S_s)^2] = \mathbb{E} \left[ \sum_{l=1}^{n+1} \sum_{i=1}^s \left[ \left( \frac{\partial \ell}{\partial B_i^{(l)}} \right)^2 \frac{i^\alpha}{\sigma_b^2(i)} + \sum_{j=1}^s \left( \frac{\partial \ell}{\partial W_{i,j}^{(l)}} \right)^2 \frac{(ij)^\alpha}{\sigma_w^2(i)} \right] \right] \quad (49)$$

to be converging, which will generally not be the case, as one can check by repeating the proof for the pCNL case (note that the likelihood contribution would have to dominate the diverging  $i^\alpha$  terms).

It remains to show that  $S_s$  is a  $L^2$ -bounded martingale. The expectation part is straightforward by the independence of the random variables involved and noting that by assumption  $\sum_{k=1}^M \frac{\partial \ell}{\partial v_k} = 0$ . We define  $g_i^{(l)}(x) = \varphi(f_i^{(l)}(x))$  to simplify notation. From (41) we get  $\mathbb{E}[(f_i^{(l)})^2] \leq \sigma_l^2/i^\alpha$ , and combining this bound with Assumption 9, we get  $\mathbb{E}[(g_i^{(l)})^2] \leq \sigma_l^2/i^\alpha$ .

We ask the reader to recall Definition 12. The partial derivatives with respect to the biases and weights can be calculated by applying the chain rule multiple times, and they are given by

$$\frac{\partial \ell}{\partial W_{1,j}^{(n+1)}} = \sum_{k=1}^M \frac{\partial v_k}{\partial W_{1,j}^{(n+1)}} \frac{\partial \ell}{\partial v_k} = \sum_{k=1}^M g_{1,j}^{(n)}(x^k) \frac{\partial \ell}{\partial v_k} \quad (50)$$

$$\frac{\partial \ell}{\partial B_1^{(n+1)}} = \sum_{k=1}^M \frac{\partial v_k}{\partial B_1^{(n+1)}} \frac{\partial \ell}{\partial v_k} = \sum_{k=1}^M \frac{\partial \ell}{\partial v_k} \quad (51)$$

$$\frac{\partial \ell}{\partial W_{i,j}^{(l)}} = \frac{\partial f_i^{(l)}}{\partial W_{i,j}^{(l)}} \frac{\partial \ell}{\partial f_i^{(l)}} = g_j^{(l-1)} \frac{\partial \ell}{\partial f_i^{(l)}} \quad l = 2 \dots n \quad (52)$$

$$\frac{\partial \ell}{\partial B_i^{(l)}} = \frac{\partial f_i^{(l)}}{\partial B_i^{(l)}} \frac{\partial \ell}{\partial f_i^{(l)}} = \frac{\partial \ell}{\partial f_i^{(l)}} \quad l = 2 \dots n \quad (53)$$

$$\frac{\partial \ell}{\partial W_{i,j}^{(1)}} = x_j \frac{\partial \ell}{\partial f_i^{(1)}} \quad (54)$$

$$\frac{\partial \ell}{\partial B_i^{(1)}} = \frac{\partial \ell}{\partial f_i^{(1)}}. \quad (55)$$

We will have to consider the following partial derivatives that show up in the ones above:

$$\frac{\partial \ell}{\partial f_i^{(l)}(x)} = \frac{\partial g_i^{(l)}(x)}{\partial f_i^{(l)}(x)} \frac{\partial \ell}{\partial g_i^{(l)}(x)} \quad l = 1 \dots n \quad (56)$$

$$\frac{\partial \ell}{\partial g_i^{(l)}(x)} = \sum_{j=1}^s \frac{\partial \ell}{\partial f_j^{(l+1)}(x)} W_{j,i}^{(l+1)} \quad l = 1 \dots n, \quad (57)$$

where in the last line we have already established the dependence of  $\frac{\partial \ell}{\partial g_i^{(l)}(x)}$  on  $s$ . Using Assumption 9, we get that

$$\left| \frac{\partial g_i^{(l)}}{\partial f_i^{(l)}} \right| \leq 1.$$

Now, for  $l = n$ , by independence:

$$\mathbb{E} \left[ \left( \frac{\partial \ell}{\partial g_i^{(l)}} \right)^2 \right] = \mathbb{E} \left[ \left( \frac{\partial \ell}{\partial f_1^{(n+1)}} W_{1,i}^{(n+1)} \right)^2 \right] \quad (58)$$

$$= \frac{\sigma_{w_{n+1}}^2}{i^\alpha} \sum_{k=1}^M \left( \frac{\partial \ell}{\partial v_k} \right)^2, \quad (59)$$

and further (again by independence), for  $l < n$ ,

$$\mathbb{E} \left[ \left( \frac{\partial \ell}{\partial g_i^{(l)}} \right)^2 \right] = \sum_{j=1}^s \mathbb{E} \left[ \left( \frac{\partial \ell}{\partial f_j^{(l+1)}} W_{j,i}^{(l+1)} \right)^2 \right] \quad (60)$$

$$= \frac{\sigma_{w_{l+1}}^2}{i^\alpha} \sum_{j=1}^s \frac{1}{j^\alpha} \mathbb{E} \left[ \left( \frac{\partial \ell}{\partial f_j^{(l+1)}} \right)^2 \right] \quad (61)$$

$$= \frac{\sigma_{w_{l+1}}^2}{i^\alpha} \sum_{j=1}^s \frac{1}{j^\alpha} \mathbb{E} \left[ \left( \frac{\partial g_j^{(l+1)}}{\partial f_j^{(l+1)}} \frac{\partial \ell}{\partial g_j^{(l+1)}} \right)^2 \right] \quad (62)$$

$$\leq \frac{\sigma_{w_{l+1}}^2}{i^\alpha} \sum_{j=1}^s \frac{1}{j^\alpha} \mathbb{E} \left[ \left( \frac{\partial \ell}{\partial g_j^{(l+1)}} \right)^2 \right]. \quad (63)$$

We can use induction to show that for  $l = 1 \dots n$ ,

$$\mathbb{E} \left[ \left( \frac{\partial \ell}{\partial g_i^{(l)}} \right)^2 \right] \leq \frac{d_l}{i^\alpha} \sum_{k=1}^M \left( \frac{\partial \ell}{\partial v_k} \right)^2, \quad (64)$$

where

$$d_l = \left( \prod_{r=l+1}^{n+1} \sigma_{w_r}^2 \right) \left( \sum_{j=1}^{\infty} 1/j^{2\alpha} \right)^{n+1-l-1}. \quad (65)$$

Putting things together, we get that (48) defines a  $L^2$  bounded martingale if  $\alpha > 1$  and  $\sum_{k=1}^M \left(\frac{\partial \ell}{\partial v_k}\right)^2 < \infty$ :

$$\begin{aligned}
\mathbb{E}[(S_s)^2] &= \mathbb{E} \sum_{l=1}^{n+1} \sum_{i=1}^s \left[ \left( \frac{\partial \ell}{\partial B_i^{(l)}} \right)^2 + \sum_{j=1}^s \left( \frac{\partial \ell}{\partial W_{i,j}^{(l)}} \right)^2 \right] \\
&= \mathbb{E} \sum_{l=1}^{n+1} \sum_{i=1}^s \left[ \left( \frac{\partial g_i^{(l)}}{\partial f_i^{(l)}} \frac{\partial \ell}{\partial g_i^{(l)}} \right)^2 + \sum_{j=1}^s \left( g_j^{(l-1)} \frac{\partial g_i^{(l)}}{\partial f_i^{(l)}} \frac{\partial \ell}{\partial g_i^{(l)}} \right)^2 \right] \\
&\leq \mathbb{E} \sum_{l=1}^{n+1} \sum_{i=1}^s \left[ \left( \frac{\partial \ell}{\partial g_i^{(l)}} \right)^2 + \sum_{j=1}^s \left( g_j^{(l-1)} \frac{\partial \ell}{\partial g_i^{(l)}} \right)^2 \right] \\
&= \sum_{l=1}^{n+1} \sum_{i=1}^s \left[ \mathbb{E} \left[ \left( \frac{\partial \ell}{\partial g_i^{(l)}} \right)^2 \right] + \sum_{j=1}^s \mathbb{E} \left[ \left( g_j^{(l-1)} \frac{\partial \ell}{\partial g_i^{(l)}} \right)^2 \right] \right] \\
&\leq \sum_{l=1}^{n+1} \sum_{i=1}^s \left[ \frac{d_l}{i^\alpha} \sum_{k=1}^M \left( \frac{\partial \ell}{\partial v_k} \right)^2 + \frac{d_l}{i^\alpha} \sum_{k=1}^M \left( \frac{\partial \ell}{\partial v_k} \right)^2 \sum_{j=1}^s \frac{\sigma_l^2}{j^\alpha} \right] \\
&\leq \sum_{k=1}^M \left( \frac{\partial \ell}{\partial v_k} \right)^2 \sum_{l=1}^{n+1} d_l \sum_{i=1}^s \left[ \frac{1}{i^\alpha} \left( 1 + \sum_{j=1}^s \frac{\sigma_l^2}{j^\alpha} \right) \right] < \infty.
\end{aligned}$$

□

#### A.5 Proof of pCNL being well-defined.

**Theorem 4.** *The preconditioned Crank-Nicolson Langevin algorithm is a well-defined MCMC algorithm in the function space setting if  $\mathcal{CD}\Phi(u) \in \text{Im}(\mathcal{C}^{1/2})$ .*

Part of this proof can be found in Beskos et al. [2017].

*Proof.* We assume that [Cotter et al., 2013, Theorem 6.2] holds. We can then check that the change of measure arising from the gradient term is absolutely continuous with respect to the measures used in Theorem 6.2 if, and only if,  $\mathcal{CD}\Phi(u) \in \text{Im}(\mathcal{C}^{1/2})$  by the Cameron-Martin Theorem Cameron and Martin [1944]. □